# University of Massachusetts Amherst ScholarWorks@UMass Amherst

Astronomy Department Faculty Publication Series

Astronomy

2008

# Evolution of the Mass Function of the Galactic Globular Cluster System

E. Vesperini University of Massachusetts - Amherst

Follow this and additional works at: https://scholarworks.umass.edu/astro\_faculty\_pubs Part of the <u>Astrophysics and Astronomy Commons</u>

**Recommended** Citation

Vesperini, E., "Evolution of the Mass Function of the Galactic Globular Cluster System" (2008). Astronomy Department Faculty Publication Series. 9. Retrieved from https://scholarworks.umass.edu/astro\_faculty\_pubs/9

This Article is brought to you for free and open access by the Astronomy at ScholarWorks@UMass Amherst. It has been accepted for inclusion in Astronomy Department Faculty Publication Series by an authorized administrator of ScholarWorks@UMass Amherst. For more information, please contact scholarworks@library.umass.edu.

# Evolution of the mass function of the Galactic globular cluster system

E.Vesperini\*

Department of Physics and Astronomy, University of Massachusetts, Amherst, MA, 01003, USA

1 February 2008

## ABSTRACT

In this work we investigate the evolution of the mass function of the Galactic globular cluster system (GCMF) taking into account the effects of stellar evolution, two-body relaxation, disk shocking and dynamical friction on the evolution of individual globular clusters. We have adopted a log-normal initial GCMF and considered a wide range of initial values for the dispersion,  $\sigma$ , and the mean value,  $\langle \log M \rangle$ . We have studied in detail the dependence on the initial conditions of the final values of  $\sigma$ ,  $\langle \log M \rangle$ , of the fraction of the initial number of clusters surviving after one Hubble time, and of the difference between the properties of the GCMF of clusters closer to the Galactic center and the properties of those located in the outer regions of the Galaxy. In most of the cases considered evolutionary processes alter significantly the initial population of globular clusters and the disruption of a significant number of globular clusters leads to a flattening in the spatial distribution of clusters in the central regions of the Galaxy. The initial log-normal shape of the GCMF is preserved in most cases and if a power-law in M is adopted for the initial GCMF, evolutionary processes tend to modify it into a log-normal GCMF. The difference between initial and final values of  $\sigma$  and  $\langle \log M \rangle$  as well as the difference between the final values of these parameters for inner and outer clusters can be positive or negative depending on initial conditions. A significant effect of evolutionary processes does not necessarily give rise to a strong trend of  $\langle \log M \rangle$ with the galactocentric distance. The existence of a particular initial GCMF able to keep its initial shape and parameters unaltered during the entire evolution through a subtle balance between disruption of clusters and evolution of the masses of those which survive, suggested in Vesperini (1997), is confirmed.

Key words: globular clusters:general – stellar dynamics

#### **1 INTRODUCTION**

Investigation of the luminosity function of the globular cluster system (hereafter GCLF) of our Galaxy and of globular cluster systems in external galaxies has been the subject of many observational works (see e.g. Secker 1992, McLaughlin 1994, Abraham & van den Bergh 1995, Kissler-Patig 1997, Harris 1991 and references therein) because of its relevance for a number of issues of great astrophysical interest, such as the formation of globular clusters, the role of the external galactic field on the evolution of their properties and the possibility of using the turnover of the GCLF as a standard candle calibrated on the values of globular cluster systems in the Local Group for the determination of the distance of external galaxies (see e.g. Jacoby et al. 1992).

The determination of the distances of external galaxies by means of the turnover of the GCLF relies on the assumed constancy of the properties of the GCLF for galaxies of different structure and type which is quite surprising: in fact, unless one advocates a scenario in which clusters in different galaxies have different initial conditions and different dynamical histories but all leading to the same final state, such common characteristics imply that the process of formation of globular clusters does not depend on the galactic environment and that evolutionary processes (tidal stripping, disk and bulge shocking, dynamical

<sup>\*</sup> E-mail:vesperin@falcon.phast.umass.edu

friction; see e.g. Meylan & Heggie 1997, for a recent review on the dynamics of globular clusters) have not played a relevant role in determining the present properties of globular clusters.

While the present knowledge of the processes leading to the formation of globular clusters is still very uncertain (see e.g. Fall & Rees 1985, Harris & Pudritz 1994, Vietri & Pesce 1995, Elmegreen & Efremov 1997) many theoretical investigations (Aguilar, Hut & Ostriker 1988, Chernoff, Kochanek & Shapiro 1986, Chernoff & Shapiro 1987, Vesperini 1994, 1997, Okazaki & Tosa 1995, Murali & Weinberg 1997, Gnedin & Ostriker 1997, Baumgardt 1998) have clearly shown that evolutionary processes should have altered significantly the initial properties of globular clusters in galaxies like the Milky Way by causing the complete disruption of a fraction of them and by altering the initial properties of the surviving ones. As it has been shown in several works (see e.g. Caputo & Castellani 1984, Chernoff, Kochanek & Shapiro 1986, Vesperini 1994, 1997, Murali & Weinberg 1997, Ostriker & Gnedin 1997, Baumgardt 1998) the inner regions of the Galaxy are those where evolutionary effects are expected to be more efficient and where to look for traces of their effects. Indeed Chernoff & Djorgovski (1989) have provided the first observational evidence of this by showing that the fraction of clusters in the post-core collapse phase increases as the distance from the Galactic center decreases. In a subsequent work Bellazzini et al. (1996) have shown the existence for clusters located in the inner regions of the Galaxy of a significant correlation between concentration and galactocentric distance in the sense of more concentrated clusters being on average closer to the Galactic center. This is likely to result from evolution (Vesperini 1994, 1997, Bellazzini et al. 1996) occuring faster for clusters located in the inner regions of the Galaxy than for those in the outer ones.

The situation concerning differences between the GCLF of inner and outer clusters is far from being clear. In a recent work Gnedin (1997) has carried out an analysis of the available observational data for clusters in the Galaxy, M31 and M87, and his results seem to point to the existence of some differences between the GCLF of inner and outer clusters for all these three galaxies: inner clusters tend to be brighter and to have smaller dispersions than outer clusters. Kavelaars & Hanes (1997) have addressed the same issue for the Milky Way and M31 and their conclusion is that, while there is no significant difference in the mean luminosity of inner and outer clusters, their distributions are actually different, the inner clusters being well described by a Gaussian in the magnitude with a dispersion significantly smaller than that of outer clusters; as for M87, Harris et al. (1998) in a recent analysis have not found any significant radial gradient in the properties of the GCLF for clusters with masses  $M > 10^5 M_{\odot}$  except for a possible trend for the dispersion of the GCLF of the innermost region of M87 that they have considered to be smaller than the dispersion of the GCLF of clusters in the outer regions of the galaxy. As discussed in Gnedin (1997) the reason for the difference between his analysis and that by Kavelaars and Hanes could reside in the different statistical methods adopted for deriving the parameters of the distribution. A trend for inner clusters to be brighter than the outer ones was previously suggested by van den Bergh (1995) and Crampton et al. (1985) for clusters in the Milky Way and in M31 respectively.

From a theoretical point of view, as we said above, this trend is consistent with that expected to result from evolutionary processes, at least for some initial GCMFs, which are more efficient in the inner regions of the Galaxy where they can efficiently disrupt low-mass clusters (see e.g. fig. 2 in Vesperini 1997). In Vesperini (1994, 1997) the evolution of the properties of a system of globular clusters located in a model of the Milky Way under the effects of relaxation, disk shocking and, in an approximate way, of dynamical friction, starting from three different initial GCMF, has been investigated. In all these cases a trend for inner clusters to be more massive than outer clusters was obtained as a result of evolutionary processes, with the extent of the difference depending on the initial GCMF chosen.

While in Vesperini (1994,1997), besides addressing some general issues on the evolution and the properties of the GCMF, we investigated the origin of some observed correlations between structural properties of individual globular clusters and between structural parameters of clusters and their position inside the host galaxy, in this work we will focus our attention on and investigate in larger detail the evolution of the properties of the GCMF of a globular cluster system located in a model for the Milky Way adopting some analytical formulae for the time evolution of the masses of individual clusters obtained by the results of a large set of N-body simulations carried out by Vesperini & Heggie (1997).

We will adopt a log-normal distribution for the initial GCMF and we will consider a wide range of different initial conditions largely spanning the space of the initial parameters (dispersion and mean) of the GCMF. Different functional forms for the initial GCMF have also been studied to investigate the evolution of their shape and in particular to establish if the current gaussian shape could result from an initial GCMF with a different functional form.

We will devote a section to the comparison of our results with observational data, but we point out that due to some assumptions made in our analysis, which will be discussed in sect.2 together with the description of the method adopted for our investigation, an exact comparison of our results with the available observational data is beyond the scope of our work. The main goal of our analysis is that of providing general indications on the evolution of the properties of the GCMF, of the spatial distribution and the fraction of the initial number of clusters surviving after one Hubble time. The evolution of the shape of the GCMF for the whole sample of clusters and the possible development of differences between the GCMF of clusters located in the inner and in the outer regions of the Galaxy will be thoroughly investigated paying particular attention to the dependence of the final results on the initial conditions. The issue, raised in Vesperini (1997), of the possible existence of a dynamical "equilibrium" GCMF able to preserve its initial shape and parameters for one Hubble time through a subtle balance between disruption of clusters and evolution of the masses of the surviving ones is further investigated.

The scheme of the paper is the following. In sect.2 the method adopted for our study is described; in section 3 we report the main results of the investigation: after a preliminary qualitative discussion on the evolution of the GCMF in section 3.1, in sections 3.2-3.6 we describe the results obtained not including the effects of disk shocking; in particular section 3.2 discusses the possible evolutionary paths of the parameters of the GCMF depending on the initial conditions (see e.g. figure 3) and the existence of a GCMF of dynamical equilibrium is shown and discussed in detail (see e.g. figure 4c), section 3.3 is focussed on the dependence of the final GCMF on the distance from the Galactic center (see e.g. figure 10 and 11), in section 3.4 the time evolution of some systems is followed in detail and some other aspects of the GCMF able to stay in dynamical equilibrium are studied (see figure 13). Section 3.5 and 3.6 are devoted to the study of the fraction of surviving clusters and their spatial distribution in the Galaxy respectively; in section 3.7 we discuss the results obtained including the effects of disk shocking. In section 4 we describe the results obtained assuming a power-law initial GCMF and section 5 is devoted to the comparison of our results with observational data. Summary and conclusions are in section 6.

#### 2 METHOD

In order to calculate the evolution of the GCMF we need to know the time evolution of the masses of individual globular clusters in the system. In this work we will adopt the analytical formulae obtained in Vesperini & Heggie (1997) which supply the mass at any time t of a cluster with initial mass  $M_i$  and moving in a circular orbit at a distance  $R_g$  from the Galactic center. These have been obtained by fitting the results of a large set of N-body simulations following the evolution of globular clusters driven by internal relaxation, stellar evolution, disk shocking and including the effects of the tidal field of the Galaxy. We summarize here for convenience the main assumptions made in the simulations carried out by Vesperini & Heggie (1997) and we refer to that paper for further details.

(i) Clusters are assumed to move on circular orbits in a Keplerian potential determined by a point mass  $M_g$  equal to the mass of the Galaxy inside the adopted galactocentric distance  $R_g$ . For the simulations including the effects of disk shocking, it is assumed that orbits cross the galactic disk perpendicularly. The circular speed has been taken equal to  $v_c = 220$  km/s.

(ii) Disk shocking has been included according to the model described in Chernoff, Kochanek & Shapiro (1986) and the same two-component disk model obtained by Chernoff et al. by a fit of the Bahcall's (1984) determination of acceleration in the solar neighbourhood has been adopted. This is an exponential isothermal disk model with scale heights equal to 175 pc and 550 pc and scale length h = 3.5 Kpc.

(iii) An initial multi-mass King model with  $W_0 = 7$  has been adopted. A set of simulations starting with  $W_0 = 5$  has been also carried out in Vesperini & Heggie (1997) and it was shown that the evolution of the total mass does not depend strongly on the initial concentration of the cluster.

(iv) The initial stellar mass function has been taken equal to a power-law  $dN(m) = m^{-2.5} dm$  between  $0.1m_{\odot}$  and  $15m_{\odot}$ .

(v) Stellar evolution is modelled following the same model used in Chernoff & Weinberg (1990) and the mass lost by each star is assumed to escape immediately from the cluster.

Fitting the results of N-body simulations not including the effects of disk shocking, Vesperini & Heggie (1997) have obtained the following expression for the time evolution of the total mass of a cluster with initial mass  $M_i$  and galactocentric distance  $R_g$ 

$$\frac{M(t)}{M_i} = 1 - \frac{\Delta M_{st.ev.}}{M_i} - \frac{0.828}{F_{cw}}t$$
(1)

where t is time measured in Myr,  $\frac{\Delta M_{st.ew.}}{M_i}$  is the mass loss due to stellar evolution (see eq.[10] in Vesperini & Heggie 1997) and  $F_{cw}$  is a parameter, introduced by Chernoff & Weinberg (1990), which is proportional to the relaxation time and defined as

$$F_{cw} \equiv \frac{M_i}{M_{\odot}} \frac{R_g}{Kpc} \frac{1}{\ln(N)} \frac{220 \text{km s}^{-1}}{v_c}$$
(2)

where  $M_i$  and N are, respectively, the initial mass and the initial number of stars in the cluster,  $R_g$  is the distance from the Galactic center and  $v_c$  the circular velocity around the Galaxy.

From the simulations including disk shocking an expression analogous to eq.(1) has been derived but with the factor  $0.828/F_{cw}$  replaced by the following factor  $\lambda$  (see Vesperini & Heggie 1997 for further details on the derivation)

$$\log \lambda = 0.6931 - 1.46 \log R_g - 1.134 \log F_{cw} + 0.2916 \log F_{cw} \log R_g.$$
(3)

A comparison of the characteristic cluster lifetime from eq.(1) with other estimates present in the literature has been made in Vesperini & Heggie (1997). More recently in an analysis of the evolution of globular cluster systems Baumgardt

(1998) has adopted a formula for the mass loss introduced by Wielen (1988) but with a new value for the numerical factor present in the original expression obtained by fitting some numerical results present in the literature; for the initial conditions considered in Vesperini & Heggie (1997) the cluster lifetime obtained by Baumgardt turns out to be 10 per cent longer than that obtained by eq. (1) without considering the mass loss associated to stellar evolution (stellar evolution is not considered in Baumgardt's analysis) while if we include the effects of stellar evolution in the estimate of the cluster lifetime derived from eq. (1), the lifetime obtained by Baumgardt is 30 per cent longer than ours.

As we have anticipated in the Introduction, in this investigation many different initial conditions for the GCMF of the system have been investigated. For any system considered,  $10^4$  random values of  $M_i$  according to the chosen initial GCMF have been calculated and a random value for the galactocentric distance from a distribution such that the number of cluster per cubic Kpc is proportional to  $R_g^{-3.5}$  has been assigned to each cluster with 1 Kpc  $< R_g < 20$  Kpc. This functional form for the number density profile is suggested by what is observed in our Galaxy between 4 Kpc  $< R_g < 20$  Kpc where the sample of observed clusters is likely to be complete (see e.g. Zinn 1985).

Once the initial conditions have been set, the GCMF at any time t can be easily calculated by means of eq. (1). In order to consider the effects of dynamical friction, clusters whose timescale of orbital decay (see e.g. Binney & Tremaine 1987) is less than t are removed from the sample at that time.

Our investigation will be focussed on initial conditions characterized by a log-normal initial GCMF; as we will see in the following sections in most cases the gaussian shape is well preserved during the entire evolution until the final state at t = 15 Gyr. The median value,  $\langle \log M \rangle$ , and the non-parametric estimate of the dispersion

$$\sigma = 0.7415(Q_{75} - Q_{25}),$$

where  $Q_{75}$  and  $Q_{25}$  are the 75th and 25th percentiles of the distribution from the final sample of surviving clusters, are the parameters used throughout the paper in order to characterize the final GCMF.

#### 3 RESULTS

#### 3.1 Preliminary remarks on the evolution of the GCMF

Before discussing in detail the results obtained, we will make some preliminary qualitative considerations on the possible evolutionary paths of the GCMF depending on the initial conditions chosen. In the following discussion we will assume a log-normal initial GCMF.

We start by noting that, for a given initial value of the cluster mass, all evolutionary processes, with the exception of mass loss associated to stellar evolution which depends only on the initial stellar mass function, are more efficient at smaller distances from the Galactic center (see e.g. Vesperini 1997); on the other hand, at a given galactocentric distance, disruption of clusters due to escape of stars through the tidal boundary is proportional to the relaxation time and thus it is more efficient for low-mass clusters while the efficiency of dynamical friction is an increasing function of the mass of the cluster. This implies that, while in any case inner regions are those where the effects of evolution are stronger, it is not obvious, *a priori*, in what direction the difference between the initial and the final GCMF and the difference between the GCMF of inner and outer clusters is to be driven by evolutionary processes; in fact, even though evolutionary processes always tend to decrease the mass of individual globular clusters, this obviously does not imply that the final mean value of the GCMF will be smaller than the initial one. Since a number of clusters will be disrupted before one Hubble time and will not be part of the final system, depending on the balance between the evolution of the masses of surviving clusters and the distribution of masses of those disrupted, the final mean value of the GCMF can be larger or smaller than the initial one.

For the initial conditions chosen in Vesperini (1997), as a result of disruption of inner low-mass clusters, the difference was always in the sense of inner clusters to be on the average more massive than the outer ones, and the final mean value of the whole sample of clusters was larger than the initial one but it is easily conceivable an initial GCMF dominated by high-mass clusters whose evolution is dominated by the effects of dynamical friction and in which the final difference between inner and outer clusters and the difference between the final and the initial mean value of the mass distribution is in the opposite sense.

As for the dispersion of the GCMF, one can anticipate that the effects of evolutionary processes is that of leading to a decrease of this if the initial GCMF contains a significant fraction both of low-mass clusters, which are mainly affected by tidal disruption, and of high-mass clusters significantly affected by dynamical friction: in this case dynamical friction and tidal disruption deplete the tails of the initial GCMF and thus make the dispersion of the sample of surviving clusters smaller. On the other hand the evolution of a distribution with a very small initial dispersion will be characterized by an increase of the dispersion, due to an asymmetric diffusion driven by the different mass loss of clusters all approximately with the same initial mass but located at different distances from the Galactic center.

We summarize in Table 1a the expected evolution of  $\langle \log M \rangle$  and  $\sigma$  under the effects of disruption by dynamical friction, disruption by evaporation, and mass loss of individual clusters that do not suffer complete disruption, each one considered separately from others. Depending on the relative efficiency of these three processes the GCMF can evolve in four different

(4)

directions as indicated in Table 1b. We can thus divide the space of initial parameters in four regions according to the way  $\langle \log M \rangle$  and  $\sigma$  evolve and we note here that if there is a common point among these four regions this will define the initial parameters of an "equilibrium" GCMF which will keep its initial parameters unaltered after one Hubble time.

#### 3.2 Evolution of the GCMF

The set of initial values for the dispersion and mean value of the GCMF,  $\sigma_i$  and  $\langle \log M \rangle_i$ , considered in our investigation is shown in figure 1a and the corresponding final values of  $\sigma$ ,  $\sigma_f$ , and of  $\langle \log M \rangle$ ,  $\langle \log M \rangle_f$ , calculated at t = 15 Gyr (hereafter by final value of any quantity we will mean that calculated at this time) are shown in figure 1b. The parameters to describe the final GCMF are estimated as described in sect.2.

Figures 2a and 2b show the contour plots of  $(\langle \log M \rangle_f - \langle \log M \rangle_i)$  and  $(\sigma_f - \sigma_i)$  in the plane  $\langle \log M \rangle_i - \sigma_i$  from which it is clear the dependence on the initial conditions of these quantities; figures 2c and 2d show the contour plots of  $\langle \log M \rangle_f$  and  $\sigma_f$  in the same plane. In figure 3 we have plotted only the curves corresponding to  $\langle \log M \rangle_f - \langle \log M \rangle_i = 0$  and  $\sigma_f - \sigma_i = 0$  which divide the plane of initial parameters in the four regions described qualitatively in section 3.1 (see Table 1b).

For low values of  $\sigma_i$  the evolution is toward larger final dispersions, while as  $\sigma_i$  increases the effects of evolution drive the system toward values of the dispersion smaller than the initial ones; the transition occurs approximately at  $\sigma_i \simeq 0.65$ . As for  $\langle \log M \rangle$ , for all the systems with  $\langle \log M \rangle_i > 5.2$  disruption by dynamical friction of high-mass clusters and mass loss of clusters without complete disruption are the dominant processes and thus  $\langle \log M \rangle_f < \langle \log M \rangle_i$ ; for  $\langle \log M \rangle_i < 5.2$ ,  $\langle \log M \rangle_f$ can be smaller than  $\langle \log M \rangle_i$  if the process of mass loss of clusters without complete disruption dominates or larger than  $\langle \log M \rangle_i$  if disruption by complete evaporation of low-mass clusters is the most important process.

The intersection of the two curves, as anticipated in section 3.1, corresponds to the initial (and final) parameters of an equilibrium GCMF; this particular GCMF (hereafter E-GCMF), as we will show in detail below, has the very interesting property of maintaining its initial shape and parameters unchanged during the entire evolution even though a significant number of clusters are disrupted because of evaporation or dynamical friction.

Figures 4a-b show the initial and the final GCMF with the corresponding gaussian fit for two typical cases of evolution of the GCMF while figure 4c shows the evolution of the E-GCMF.

It is important to note from this figure that all the final GCMFs shown are still well described by a gaussian distribution. This result, as pointed out in Vesperini (1997), is far from being obvious given the large number of clusters undergoing disruption during one Hubble time in most of the cases considered.

The qualitative scenario anticipated in section 3.1 is now clearly shown in figure 4: in GCMFs initially dominated by low-mass clusters the low-mass tail is significantly depleted and the final value of  $\langle \log M \rangle$  is larger than the initial one (figure 4a); for initial GCMFs dominated by high-mass clusters the evolution is in the opposite direction as the high-mass tail is that more affected by evolutionary processes and the final value of  $\langle \log M \rangle$  is smaller than the initial one (figure 4b). Figure 4c shows the E-GCMF: while, as it is evident from the figure, the final number of clusters in the system is significantly smaller than the initial one (about 52 per cent of the clusters initially in the system are disrupted) the shape and the parameters of the GCMF are almost exactly preserved after one Hubble time through the balance between disruption of clusters and evolution of the masses of those which survive. The initial dispersion and mean value of the GCMF having this interesting characteristic are  $\sigma \simeq 0.64$  and  $\langle \log M \rangle \simeq 4.93$ . The agreement with the values for the equilibrium GCMF obtained by Vesperini (1997) ( $\sigma \simeq 0.5$  and  $\langle \log M \rangle = 5.0$ ; see his GAU2 simulation) is quite remarkable given the differences in the method adopted for the investigation in that and in the present work and the fact that in Vesperini (1997) no systematic investigation of different initial conditions were done to locate the exact parameters of the equilibrium GCMF. Figure 5 shows the distribution of log  $M_i$  of those clusters in the E-GCMF which at t = 15 Gyr have  $\log M_f \simeq \langle \log M \rangle_f$  and it clearly illustrates that the equilibrium is preserved dynamically.

#### 3.3 Dependence of the GCMF on the galactocentric distance

As we discussed in the introduction, investigation of the possible differences between the properties of clusters located closer to the Galactic center and the properties of those in the outer regions of the Galaxy is of particular interest because it can provide important clues on the actual role of evolutionary processes in determining the present properties of globular clusters and on the reliability of the distances of external galaxies estimated by using the turnover magnitude of the GCLF of their globular cluster systems.

In our investigation we have classified as inner clusters all those at a distance from the Galactic center,  $R_g$ , smaller than 8 Kpc and as outer clusters all those having  $R_g > 8$  Kpc.

First we focus our attention on the difference,  $\Delta \langle \log M \rangle_{in-out} = \langle \log M \rangle_{inner} - \langle \log M \rangle_{outer}$ , between the mean value of the GCMF of inner clusters,  $\langle \log M \rangle_{inner}$ , and that of the GCMF of outer clusters,  $\langle \log M \rangle_{outer}$ .

Figure 6 shows the plot of  $\Delta \langle \log M \rangle_{in-out}$  versus  $\langle \log M \rangle_i$ . Depending on the initial conditions,  $\Delta \langle \log M \rangle_{in-out}$  can be positive or negative: all systems with  $\langle \log M \rangle_i < 4.9 - 5.1$ , the exact value depending on  $\sigma_i$ , have, after one Hubble time,

 $\langle \log M \rangle_{outer} < \langle \log M \rangle_{inner}$  while the opposite trend is established by evolutionary processes for systems initially dominated by massive clusters. The qualitative explanation for the observed behaviour of  $\Delta \langle \log M \rangle_{in-out}$  is similar to that discussed for the difference between the final and the initial value of  $\langle \log M \rangle$  for the whole sample of clusters and in fact, as shown in figure 7, there is an evident correlation between  $\Delta \langle \log M \rangle_{in-out}$  and  $\langle \log M \rangle_f - \langle \log M \rangle_i$ : the reason for this is clear if one considers that the properties of outer clusters are in general expected to resemble those of the initial system while inner clusters are likely to be those mainly responsible for the variation of the properties of the cluster system since they are more affected by evolutionary processes.

We point out that most of the systems considered evolve significantly, undergoing a strong depletion of their initial number of clusters, but in many cases the difference  $\Delta \langle \log M \rangle_{in-out}$  induced by evolutionary processes is not very large and it is easily conceivable that its observational detection can be difficult. We will return to this point below in this section and in section 5 when we will compare our results to observational data for the Milky Way.

For most of the initial conditions considered in this study, evolutionary processes tend to make the dispersion of the sample of inner clusters smaller than that of outer clusters and this is consistent with the results of the analysis of observational data for the Galaxy, M31 and M87 by Gnedin (1997) and Kavelaars & Hanes (1997). Only for systems initially characterized by a low dispersion ( $\sigma_i < 0.5$ ) the opposite trend is established in the course of evolution as it is clear from figure 8 which shows the plot of  $\Delta \sigma_{in-out}$  versus  $\sigma_i$ . This result can be easily interpreted if, as already discussed in section 3.1, one considers that for a GCMF with initial dispersion large enough, evolutionary processes, more efficient in the inner regions, tend to deplete more efficiently the low-mass tail (by tidal disruption) and the high-mass tail (by dynamical friction) of the initial distribution thus causing it to become narrower as evolution goes on.

While the above analysis based on the division of a cluster population in two subpopulations of inner and outer clusters allows to easily obtain a general quantitative measure of the radial variation of the properties of a GCMF, it is also important to study some cases more in detail and to address the issue of the radial variation of the GCMF by making a finer division of clusters according to their distance from the Galactic center and studying the properties of GCMF in more than two radial bins. Thus we discuss now in some detail to what extent a correlation between the galactocentric distance  $R_g$  and the mean mass  $\langle \log M \rangle_{R_g}$  and dispersion  $\sigma_{R_g}$  of clusters located in spherical shells with limits  $R_g - \Delta R_g$  and  $R_g + \Delta R_g$  can be produced by evolutionary process. No significant correlation between  $R_g$  and  $\langle \log M \rangle_{R_g}$  is observed in many galaxies (see e.g. Harris et al. 1998, Forbes, Brodie & Hucra 1997, Forbes et al. 1996a,b), and this result is often interpreted as an indication that evolutionary processes do not play a relevant role in the evolution of globular cluster systems.

We will show that a strong effect of evolutionary processes does not necessarily imply the formation of a strong radial gradient of  $\langle \log M \rangle_{R_q}$ .

We focus our attention on three different initial log-normal GCMF among those considered in section 3.2:

- (a)  $\langle \log M \rangle_i = 4.6, \, \sigma_i = 0.9;$
- (b)  $\langle \log M \rangle_i = 5, \sigma_i = 0.7;$
- (c)  $\langle \log M \rangle_i = 5.8, \sigma_i = 0.9.$

Initial conditions (a) and (c) have been chosen because they are among those more significantly affected by evolutionary processes since they contain many low-mass and many high-mass clusters respectively, while (b), besides being a system undergoing a significant disruption and decrease in the total number of clusters, is an initial condition which could be similar to that of the Galactic globular cluster system (see sect. 5). As shown in fig.4 (panels a and b) where the initial and the final GCMF corresponding to the initial conditions (a) and (c) are plotted (the evolution of the system (b) is not shown in figure 4 but the initial conditions and the evolution are very similar to those shown in fig. 4c for the E-GCMF), in all these three cases evolutionary processes play a significant role leading to the disruption of a significant number of globular clusters. Figure 9, in which we have plotted the initial and the final histogram of  $R_g$  for these three systems, clearly shows the depletion of clusters in the inner regions of the Galaxy.

Figure 10 shows the plot of  $\langle \log M \rangle_{R_g}$  and  $\sigma_{R_g}$  versus  $R_g$ .  $\langle \log M \rangle_{R_g}$  and  $\sigma_{R_g}$  have been calculated in five different radial bins each one including clusters between  $R_g - 1.9$  Kpc and  $R_g + 1.9$  Kpc with  $R_g = 2.9, 6.7, 10.5, 14.3, 18.1$ . It is evident that a significant disruption of clusters is not necessarily followed by the formation of a strong radial trend of  $\langle \log M \rangle_{R_g}$ ; as we pointed out above, initial conditions (a) and (c) are two rather extreme cases unlikely to be relevant for real globular cluster systems and they have been chosen because they are probably those able to give rise to the strongest radial gradient of  $\langle \log M \rangle_{R_g}$ . Initial condition (b), which is likely to be a more realistic choice for the initial GCMF, does not have a strong radial gradient of  $\langle \log M \rangle_{R_g}$ . Moreover we point out that the detection of any radial gradient of  $\langle \log M \rangle$  in globular cluster systems of external distant galaxies is likely to be more difficult if the sample of clusters observed in distant galaxies does not include the low-mass tail of the GCMF. This is clear from figure 11 where we have plotted  $\langle \log M \rangle_{R_g}$  versus  $R_g$  for the case (a) as in figure 10 but excluding the low-mass tail of the GCMF beyond  $1\sigma$ : the trend present when the complete population of clusters is considered, disappears when the low-mass tail of the distribution is excluded. Finally we note that, since we have considered only circular orbits, we expect any radial gradient in our theoretical sample to be stronger than the corresponding one derived by observational data where the current values of the galactocentric distances do not necessarily provide an exact indication of the galactic tidal field affecting clusters; this, of course, does not mean that no gradient at all is expected when non-circular orbits are considered and in fact Murali & Weinberg (1997) and Baumgardt (1998), who include non-circular orbits in their analysis, find that evolutionary processes give rise to a radial trend in the properties of the mass distribution with clusters on more eccentric orbits being in general those more easily disrupted. The situation is even more unfavourable to the detection of a radial gradient when, as in the case of globular clusters in external galaxies, observational data provide projected distances from the galactic center.

In conclusion while in principle evolutionary processes are expected to induce a radial gradient in the mean mass of globular clusters, in practice the extent of this depends significantly on initial conditions and in some cases, even though evolutionary processes are very efficient and a significant number of clusters are disrupted, the radial gradient of  $\langle \log M \rangle$  is very weak.

#### 3.4 Time evolution of the GCMF

While in the previous sections we have focussed our attention on the final properties of the GCMF and investigated their dependence on the initial conditions, in this section we will study the time evolution of the parameters of the GCMF by showing and discussing some typical "paths" followed by the properties of the GCMF from t = 0 to t = 15 Gyr.

The rate of evolution of the GCMF properties is determined by the rate of disruption of clusters and the rate of change of the masses of those which survive. Mass loss by stellar evolution depends on time and it is significant only for t < 1Gyr (see e.g. Vesperini & Heggie 1997) when more massive stars evolve out of the main sequence; as for disruption by evaporation and by dynamical friction, since, for a given mass, inner clusters are those expected to be more affected by these evolutionary processes, the rate of evolution of the GCMF is to depend on the number of clusters closer to the Galactic center; as time goes on and the "weaker" clusters closer to the Galactic center are disrupted by evaporation or dynamical friction, the number of clusters liable to the effects of these processes on relatively short time scales decreases and eventually the rate of change in GCMF parameters slows down.

Figures 12a-c, where we have plotted the time evolution of  $\langle \log M \rangle$ , of  $\sigma$  and of the ratio of the total number of clusters in the system at time t to the total initial number of clusters clearly show this effect: after a phase of significant change in  $\langle \log M \rangle$  and  $\sigma$ , as mass loss by stellar evolution ceases to be important and the number of clusters in the inner regions of the Galaxy has decreased, the evolution of the parameters of the GCMF slows down significantly.

It is important to note the difference between the equilibrium reached due to a more "favourable" spatial distribution and the more interesting E-GCMF discussed in section 3.2 which remains unchanged since the beginning in dynamical equilibrium independent on the underlying spatial distribution.

Figure 13 further clarifies this point by clearly showing the existence of a particular GCMF able to stay in equilibrium for one Hubble time. The trajectories shown in figure 13 are determined in the following way: for a given initial condition an arrow joins the initial conditions in the plane  $\sigma$ - $\langle \log M \rangle$  to the corresponding values after 15 Gyr, these final values of  $\sigma$  and  $\langle \log M \rangle$  are then used as initial conditions for the following step in which, again, an arrow joins these new initial conditions to the corresponding final values and so on. It is important to realize that the trajectory obtained in this way is not a real trajectory in the plane  $\sigma$ - $\langle \log M \rangle$  since each time a new step is done, the starting point of the new step is the final state of the previous one but the underlying changes in the spatial distribution of clusters in the Galaxy and in the stellar mass function of individual globular clusters, which cause the slowing down of the evolution, are eliminated; thus the system restarts with the full spatial distribution, each cluster loses mass by stellar evolution according to the complete initial stellar mass function and a new impulse is given to the motion in the  $\sigma$ - $\langle \log M \rangle$ . In this sense the E-GCMF is an attractor in the plane  $\sigma$ - $\langle \log M \rangle$ since it is the only GCMF which, taken as an initial condition, does not need any particular spatial distribution and the decrease of mass loss associated to stellar evolution to slow the rate at which its parameters evolve; as discussed above, these preserve their initial values unaltered for a Hubble time due to the balance between disruption of clusters and evolution of the masses of those which survive.

#### 3.5 Fraction of surviving clusters

One interesting issue concerning the Galactic globular cluster system is the relationship between their present number, their present total mass and the corresponding initial values of these quantities. As expected, the fraction of surviving clusters and the ratio of the total present mass of clusters to the initial one depend significantly on the initial conditions. Figures 14a and 14b show the contour plot of the ratio of the total number of clusters surviving after 15 Gyr to the total initial number of clusters,  $F_N$ , and of the ratio of the total mass of all surviving clusters after 15 Gyr to the total initial mass of all clusters,  $F_M$ , in the plane  $\sigma_i$ - $\langle \log M \rangle_i$ .

For a given value of  $\sigma_i$ ,  $F_N$  ( $F_M$  has a similar behaviour) has a maximum for the value of  $\langle \log M \rangle_i$ ,  $\langle \log M \rangle_{max}$ , corresponding to the most "robust" initial GCMF which is that having the minimum number of clusters undergoing disruption by evaporation (low-mass clusters) or by dynamical friction (high-mass clusters); the increasing number of low-mass clusters

(easily disrupted by evaporation), for  $\langle \log M \rangle_i < \langle \log M \rangle_{max}$  and of high-mass clusters (undergoing disruption by dynamical friction) for  $\langle \log M \rangle_i > \langle \log M \rangle_{max}$  explains the observed decrease of  $F_N$ .

Figure 14 gives an indication on the total number of clusters disrupted in one Hubble time but it is also interesting to estimate the current disruption rate,  $F_D$ , defined as the fraction of the number of clusters at t = 15 Gyr undergoing disruption in the next 1 Gyr

$$F_D = \frac{N_{gc}(15) - N_{gc}(16)}{N_{gc}(15)} \tag{5}$$

where  $N_{gc}(t)$  indicates the total number of clusters at time t (in Gyr). Hut & Djorgovski (1992) by an analysis of the distribution of the half-mass relaxation times of Galactic clusters have estimated  $F_D \simeq 0.038 \pm 0.02$ . Figure 15 shows the contour plot of  $F_D$  in the plane  $\sigma_i \cdot \langle \log M \rangle_i$ . It is interesting to note that for the values of  $\sigma_i$  and of  $\langle \log M \rangle_i$  which are likely to be relevant for the Galactic globular cluster system ( $\langle \log M \rangle \simeq 5$  and  $\sigma \simeq 0.7$ ) the values of  $F_D$  we obtain are very close to that obtained by Hut & Djorgovski (1992).

#### 3.6 Spatial distribution

In section 3.4 we have already made some comments on the evolution of the spatial distribution of clusters in the Galaxy, pointing out that the larger efficiency of evolutionary processes in the inner regions of the Galaxy tends to flatten the profile of number density of clusters close to the galactic center. In the outer regions the fraction of disrupted clusters is in most cases negligible and the initial power-law profile with index equal to -3.5 is preserved. In order to provide a quantitative measure of the flattening in the density profile acquired during the evolution as a function of the initial conditions we have calculated the core radius  $R_c$  by fitting the final number density profile for all the cases investigated with the following function (see, e.g. Djorgovski & Meylan 1994)

$$n(R_g) = A \left(1 + R_g/R_c\right)^{-3.5} \tag{6}$$

We note that for the initial conditions  $n(R_g) \propto R_g^{-3.5}$  between  $R_g = 1$  Kpc and  $R_g = 20$  Kpc a fit of the initial number density by eq. (6) results in a very small core radius ( $R_c \simeq 0.1$  Kpc).

The contour plot of  $R_c$  in the plane  $\sigma_i \cdot \langle \log M \rangle_i$  is shown in fig.16. In all the cases investigated the spatial distribution tend to flatten in the inner regions of the Galaxy and the effect is stronger (larger values of  $R_c$ ) for initial conditions containing many low-mass clusters (efficiently disrupted by evaporation) or many high-mass clusters (efficiently disrupted by dynamical friction).

#### 3.7 Inclusion of disk shocking

All the simulations discussed in the previous section do not include the effects of disk shocking. In the light of the results obtained by Vesperini & Heggie (1997) concerning the difference between the time evolution of the total mass with and without disk shocking, it is obvious to expect some quantitative differences in the final results once the effects of disk shocking are included but all the general conclusions concerning the trends and the dependence of the final results on the initial conditions, the existence of an equilibrium GCMF, the definition of different regions in the plane of initial conditions are unaltered.

Since, as discussed in Vesperini & Heggie (1997), the analytical expression providing the time evolution of the total mass of a cluster as a function of its galactocentric distance and its initial mass is more approximate and is valid for a smaller range of initial parameters than the corresponding one without the effects of disk shocking, we have adopted this formula only for clusters with  $R_g < 8$  Kpc assuming the effects of disk shocking at larger galactocentric distances to be negligible.

Figures 17a-d show the plots of the final values of  $\langle \log M \rangle$ ,  $\sigma$ ,  $F_N$  and  $F_D$  from the runs not including disk shocking versus the corresponding values ( $\langle \log M \rangle_{f,ds}, \sigma_{f,ds}, F_{N,ds}, F_{D,ds}$ ) obtained from the simulations including disk shocking. As expected in all cases the number of surviving clusters is smaller when disk shocking is included but  $F_N - F_{N,ds}$  is never larger than  $0.2F_N$  and in most cases is smaller than  $0.1F_N$ . As for  $\langle \log M \rangle$  and  $\sigma$  we obtain  $-0.015 < (\langle \log M \rangle_{f,ds} - \langle \log M \rangle_f) / \langle \log M \rangle_f < 0.013$  and  $-0.12 < (\sigma_{f,ds} - \sigma_f) / \sigma_f < 0.07$ .

For what concerns the parameters of the equilibrium GCMF we obtain  $(\log M)_i \simeq 5.03$ ,  $\sigma \simeq 0.66$  quite close to the corresponding values obtained without disk shocking ( $(\log M)_i \simeq 4.93$ ,  $\sigma \simeq 0.64$ ).

# 4 DIFFERENT INITIAL GCMF

A complete theory of the process of globular cluster formation is still lacking and the only support for a log-normal initial GCMF comes from the observations of the present GCMF. While assuming such a functional form also for the initial GCMF is a reasonable guess it is interesting to consider other possibilities.

In some works it has been suggested that the initial GCMF could be a power-law in M (see e.g. Harris & Pudritz (1994),

Elmegreen & Efremov (1997) and also Elemegreen & Efremov (1997) for references to past observational and theoretical analysis on this issue) and observations of the luminosity function of young clusters in interacting galaxies (see e.g. Whitmore & Schweizer (1995) for NGC 4038/39) show a GCLF which is a power law in L (but see Fritze-v.Alvensleben (1998), for a recent interesting analysis determining the intrinsic mass distribution of young clusters in NGC 4038/39 and showing this to be a log-normal distribution; see also Meurer (1995)). Thus we have considered this possibility and investigated the evolution of systems with an initial GCMF given by

$$f(M) = AM^{-\alpha} \text{ for } M_{low} < M < M_{up} \tag{7}$$

with  $\alpha = 2, 1.7, 1.5, M_{up}(M_{\odot}) = 10^{6.5}$  and  $M_{low}(M_{\odot}) = 10^3, 10^{3.5}, 10^4, 10^{4.5}, 10^5, 10^{5.5}$ . In agreement with the results of previous analysis (see e.g. Okazaki & Tosa 1995, Vesperini 1994, 1997, Baumgardt 1998) we obtain that in all these cases evolutionary processes tend to modify the initial power-law GCMF in a bell-shaped GCMF when binned in log M. In figure 18 the initial and the final GCMF for the case  $(M_{low} = 10^4 M_{\odot}, \alpha = 2)$  are shown: it is evident that evolutionary processes are very efficient in modifying the initial GCMF into a log-normal distribution. As  $M_{low}$  increases the evolution of the mass of individual surviving clusters occurs on longer timescales and thus the process of asymmetric diffusion (see section 3.1) which is responsible for the formation of the low-mass tail in the final GCMF is slower; consequently, even though the tendency of the GCMF to evolve toward a bell-shaped distribution in log M persists, the deviations of the GCMF at t = 15 Gyr from a log-normal distribution increases for larger values of  $M_{low}$ .

Figures 19a-b show the plots of  $\langle \log M \rangle$  and  $\sigma$  of the final GCMF (defined as described in sect. 2 also for the cases in which the final GCMF deviates significantly from a log-normal distribution) versus  $\log M_{low}$  for the values of  $\alpha$  considered. It is interesting to note the existence of two regimes: for small values of  $M_{low}$  ( $M_{low} < 10^{4.5} M_{\odot}$ ), the final value of  $\langle \log M \rangle$  and  $\sigma$  do not depend on  $M_{low}$  and they are determined by evolutionary processes and by the value of  $\alpha$ ; for  $M_{low} > 10^{4.5} M_{\odot}$ ,  $\langle \log M \rangle$  and  $\sigma$  are essentially determined by the value of  $M_{low}$  and  $\langle \log M \rangle$  keeps memory of the initial value of  $M_{low}$  (in fact it is approximately equal to  $\log M_{low}$ ).

#### 5 COMPARISON WITH OBSERVATIONAL DATA

As we discussed in the introduction a detailed comparison of our theoretical results with observational data is beyond the scope of this work both because of some limitations in our analysis and because of the uncertainties in the initial conditions to adopt for the Galactic globular cluster system. Nevertheless, while keeping these caveats in mind, it is interesting to see to what extent the predictions of our analysis are in general consistent with some of the observed properties of the Galactic globular cluster system.

Real initial conditions of the Galactic globular cluster system are unknown but a reasonable assumption is that of looking at the properties of clusters in the outer regions of the Galaxy, where evolutionary processes act on longer timescales, and adopting these as initial conditions for the entire cluster system (see also Fall & Malkan 1978 for an interesting study aimed to obtain information on the initial distribution of globular cluster core properties from the current observational data). From the estimate of the mean magnitude and dispersion of the current GCLF for galactic halo clusters with  $R_g > 8$  Kpc obtained by Gnedin (1997) (see his table 1), assuming  $M/L_V = 2$ , the following values are obtained:  $\langle \log M \rangle_i = 5.0, \sigma_i = 0.7$ . Assuming an initial log-normal GCMF with these parameters we have calculated some quantities that can be compared with observational data.

The results of this calculation, summarized in Table 2, are in general in good agreement with the observational data.

In agreement with the analysis by Kavelaars & Hanes (1997), Gnedin (1997) and Ostriker & Gnedin (1997), we find that the dispersion of inner clusters is smaller than that of outer clusters; as for the difference between  $\langle \log M \rangle$  of inner and outer we find  $\langle \log M \rangle_{inner} > \langle \log M \rangle_{outer}$  in agreement with the conclusion of Gnedin (1997) and Ostriker & Gnedin (1997).

According to our results the current number of clusters would be about half ( $F_N = 0.54$  if disk shocking is not considered and  $F_N = 0.48$  taking into account the effects of disk shocking) of the total initial number of clusters and the total current mass would be about 40 per cent of the total initial mass. This implies that the total initial number of clusters in our Galaxy would be about 300 and their total initial mass about  $9 \times 10^7 M_{\odot}$  (where we have adopted  $M/L_V = 2$  and the values of the total visual magnitude of Galactic clusters tabulated in Djorgovski 1993) from which it follows that the contribution to the halo mass from disrupted clusters and stars escaped from survived clusters would be about  $5.5 \times 10^7 M_{\odot}$  a value very far from being able to account for the entire halo mass.

Figure 20 shows the histogram of the ratio of the current to initial masses of surviving clusters (the effects of disk shocking are considered) providing us with an interesting information on the relationship between the initial and the final state of surviving clusters. The bin  $0.9 < M_f/M_i < 1$  is empty since all clusters lose about 18 per cent of their initial mass due to the mass loss associated to the stellar evolution; this means that clusters from which no star escapes have  $M_f/M_i \simeq 0.82$  and they are in the bin  $0.8 < M_f/M_i < 0.9$ . It is interesting to note that, even though the masses of many surviving clusters are quite close to their initial values, there are several clusters which have lost a significant fraction of their initial mass; for

about 40 per cent of the surviving clusters the current mass is less than half the initial mass. As discussed in Vesperini & Heggie (1997) the stellar IMF of these clusters evolves significantly and a significant fraction of their current mass is expected to be in white dwarfs and thus they are object of great interest; unfortunately most of them are likely to be located in the inner regions of the Galaxy and they are challenging targets for observations.

We conclude this section discussing the issue of the distribution of the disruption timescale  $t_d(t)$ , defined as the time necessary for the complete disruption of a cluster at a time t after its formation.

In a recent investigation Gnedin & Ostriker (1997) have addressed this point and have estimated the destruction rate for 119 Galactic globular clusters taking into account the current observed properties of the clusters considered.

As discussed in detail in Gnedin & Ostriker (1997), assuming that all clusters were formed at the same time  $t_0 \simeq 0$  the number of clusters surviving at time t is equal to the number of clusters for which the initial value of  $t_d$  was larger than t and the current distribution of disruption timescales is connected to the initial one by the simple relation  $f(t_d, t_H) = f_i(t_d + t_H)$ , where  $f_i$  denotes the initial distribution of the disruption timescales.

In figure 21a we show the histogram of  $\log(t_d(t_H)/t_H)$  which we have obtained for the sample of clusters surviving at  $t_H$  from an initial population with a GCMF equal to that adopted above in this section for the comparison of our data with observational data. The effects of stellar evolution, disk shocking, two-body relaxation and dynamical friction have been considered and, for ease of later comparison with the results of the analysis of Gnedin & Ostriker, the Hubble time has been taken equal to  $t_H = 10$  Gyr.

If, as suggested by Gnedin & Ostriker (1997), we make the hypothesis that the initial distribution of  $t_d$  is a power-law,  $f_i(t_d) \sim t_d^{-q}$ , from the median value of  $t_d$  in our sample we estimate  $q \simeq 1.6$  which falls in the range of the values obtained by Gnedin & Ostriker and as shown in figure 21a (dashed line) this distribution fits fairly well the data. On the other hand, since in our analysis we know the real initial conditions we can calculate the initial distribution of  $t_d$  and verify the hypothesis made. In figure 21b the distribution of  $t_d(t = 0)$  is shown and it is evident that the initial distribution is not a power-law, but it is well fitted by a log-normal distribution; as expected, adopting this functional form for  $f_i(t_d)$  a much better fit is obtained for  $f(t_d, t_H)$  (solid line in figure 21a).

We conclude emphasizing that much caution is needed in drawing any conclusion on the initial number and initial properties of clusters on the basis of the current distribution of disruption times; as shown in fig.22, in fact, the differences in  $f(t_d, t_H)$  derived from three very different initial populations can be quite small and even a small uncertainty in the estimates of the parameters of the current distribution of timescales, or in the timescales themselves, can lead to a large error in the estimate of the parameters of the initial population of clusters.

#### 6 SUMMARY AND CONCLUSIONS

In this work we have investigated the evolution of the mass function of a globular cluster system located in a model for the Milky Way. The effects of stellar evolution, two-body relaxation, disk shocking, dynamical friction and the presence of the tidal field of the Galaxy have been taken into account in the evolution of the mass of individual globular clusters in the system which is calculated on the basis of the results of the *N*-body simulations carried out by Vesperini & Heggie (1997).

A log-normal and a power-law initial GCMF have been considered. The main effort has been devoted to the investigation of systems starting with an initial log-normal GCMF spanning a wide range of values of the mean value and the dispersion of the initial distribution. The gaussian shape has been shown to be preserved very well during the entire evolution until t = 15Gyr while for systems in which the initial GCMF is a power-law a bell-shaped GCMF resembling a Gaussian in log M tends to be established in the course of evolution.

Depending on the initial GCMF parameters, the mean value of the GCMF,  $\langle \log M \rangle$ , can increase or decrease during the evolution according to whether the dominant process is that of disruption of low-mass clusters by evaporation of stars through the tidal boundary (for initial GCMF dominated by low-mass clusters) or that of disruption by dynamical friction of high-mass clusters (for initial GCMF dominated by high-mass clusters). The regions in the space of initial parameters  $\langle \log M \rangle_i$ - $\sigma_i$  corresponding to these two different regimes as well as the corresponding regions for the evolution of the dispersion  $\sigma$  has been shown.

The differences between the final values of  $\langle \log M \rangle$ ,  $\Delta \langle \log M \rangle_{in-out}$ , and  $\sigma$ ,  $\Delta \sigma_{in-out}$ , of inner ( $R_g < 8$  Kpc) and outer clusters ( $R_g > 8$  Kpc) have been investigated. Depending on the dominant evolutionary process (disruption of low-mass clusters or dynamical friction)  $\Delta \langle \log M \rangle_{in-out}$  can be larger or smaller than zero. As for  $\Delta \sigma_{in-out}$ , in most cases considered evolutionary processes tend to make the dispersion of inner clusters smaller than that of outer clusters. The formation of a gradient of  $\langle \log M \rangle$  and  $\sigma$  with the galactocentric distance due to evolutionary processes has been investigated. The direction of the gradient of  $\langle \log M \rangle$  depends on the initial GCMF: an increasing  $\langle \log M \rangle$  as  $R_g$  increases is common for systems initially containing many high-mass clusters while the opposite trend is typical of systems initially dominated by low-mass clusters. It has been shown that a significant effect of evolutionary processes does not necessarily imply the formation of a strong radial trend of  $\langle \log M \rangle$ . For most initial conditions considered, and in particular for those likely to be relevant for real systems, evolutionary processes give rise to a trend for  $\sigma$  to decrease at smaller galactocentric distances.

The existence of a particular GCMF able to stay in dynamical equilibrium keeping its initial shape and parameters unaltered during the entire evolution by means a subtle balance of disruption of clusters and evolution of the masses of those surviving, first suggested by Vesperini (1997), has been confirmed.

The initial number density distribution of clusters in the Galaxy has been taken proportional to  $R_g^{-3.5}$  and it has been shown that evolutionary processes tend to flatten this distribution close to the Galactic center. The extent of the flattening depends on the initial conditions and it has been estimated quantitatively by calculating the final core radius,  $R_c$ , of the distribution of survived clusters in the Galaxy. The range spanned by  $R_c$  for the initial conditions considered in our work is 0.4 - 2 Kpc.

The fraction of the total initial number of clusters surviving after one Hubble time,  $F_N$ , the fraction of the total initial mass of all the clusters in the system,  $F_M$ , and the current cluster disruption rate (defined as the fraction of the number of clusters at t = 15 Gyr undergoing disruption within the next 1 Gyr), have been calculated and their dependence on the initial conditions investigated.

The exact comparison of our results with observational data is beyond the scope of our work both because of some simplifying assumptions we have made and because of the current lack of a precise knowledge of the initial properties of the Galactic globular cluster system; nevertheless assuming the current properties of outer clusters to be similar to the initial ones of the entire system we have calculated the values predicted from our analysis for some of the observed properties of the Galactic globular cluster system and we have found them to be in general in good agreement with the observational values.

As for the fraction of the total initial number of cluster surviving at the current epoch,  $F_N$ , and the fraction of the total initial mass of all the globular clusters,  $F_M$ , the values predicted for the Galactic system are  $F_N \simeq 0.54$  (0.48 if the effects of disk shocking are included) and  $F_M \simeq 0.41$  (0.38 with disk shocking). These values imply that the initial population of Galactic globular clusters would consist of about 300 clusters with a total mass of about  $9 \times 10^7 M_{\odot}$  and that the contribution to the halo mass from disrupted clusters and stars escaped from survived clusters would be about  $5.5 \times 10^7 M_{\odot}$ . The distribution of clusters disruption times has been calculated and shown to be similar to the distribution of disruption times for a sample of 119 Galactic clusters obtained by Gnedin & Ostriker (1997); we have shown that very different initial distributions of disruption timescales can lead to very similar final distributions and thus much caution is necessary in drawing any conclusion on the initial population of clusters from the present distribution of disruption timescales.

#### ACKNOWLEDGMENTS

I wish to thank Giuseppe Bertin and Rainer Spurzem for many useful comments on this paper and D.C.Heggie and M.D.Weinberg for many useful and enlightening discussions.

### REFERENCES

Abraham R.G., van den Bergh S., 1995, ApJ, 438, 218 Aguilar L., Hut P. Ostriker J.P. 1988, ApJ, 335, 720 Bahcall J.N., 1984, ApJ, 287, 926 Baumgardt H., 1998, A&A, 330, 480 Bellazzini M., Vesperini E., Ferraro F.R., Fusi Pecci F., 1996, MNRAS, 279,337 Binney J., Tremaine S., 1987, Galactic Dynamics, Princeton University Press, Princeton, New Jersey Caputo F., Castellani V., 1984, MNRAS, 207,185 Chernoff D.F., Kochanek C.S., Shapiro S.L., 1986, ApJ, 309, 183 Chernoff D.F. & Shapiro S.L., 1987, ApJ, 322, 113 Chernoff D.F., Djorgovski S.G., 1989, ApJ, 339, 904 Chernoff D.F., Weinberg M.D., 1990, ApJ, 351, 121 Crampton D., Cowley A.P., Schade D., Chayer P., 1985, ApJ, 288, 494 Djorgovski S.G., 1993 in Structure and Dynamics of Globular Clusters, Djorgovski S.G., Meylan G. Eds., Astron. Soc. of the Pac. Conf. Series vol.50, p. 373 Djorgovski S.G., Meylan G., 1994, AJ, 108, 1292 Elmegreen, B. G., Efremov, Y., 1997, 480, 235 Fall S.M., Malkan M.A., 1978, MNRAS, 185, 899 Fall S.M., Rees M.J., 1985, ApJ, 298, 18 Forbes D.A., Franx M., Illingworth G.D., Carollo C.M., 1996a, ApJ, 467, 126 Forbes D.A., Brodie J.P., Hucra J., 1996b, AJ, 112, 2448

Forbes D.A., Brodie J.P., Hucra J., 1997, AJ, 113, 887

Fritze-v.Alvensleben U., 1998, preprint, astro-ph 9803139

Gnedin O.Y., 1997, ApJ, 487, 663

Gnedin O.Y., Ostriker J.P., 1997, ApJ, 474, 223

Harris W.E., 1991, ARAA, 29, 543

Harris W.E., Pudritz R.E., 1994, ApJ, 429, 177

Harris W.E., Harris G.L.H., McLaughlin D.E., 1998, preprint, astro-ph 9801214

Hut P., Djorgovski S.G., 1992, Nature, 359, 806

Jacoby G.H., et al. 1992, PASP, 104, 599

Kavelaars J.J., Hanes, D.A., 1997, MNRAS, 285, L31

Kissler-Patig, M., 1997, A&A, 319,83

McLaughlin D.E., 1994, PASP, 106, 47

Meurer G.R., 1995, Nature, 375, 742

Meylan G., Heggie D.C., 1997, A&A Rev., 8, 1

Murali C, Weinberg M.D., 1997, MNRAS, 291, 717

Okazaki, T., Tosa, M., 1995, MNRAS, 274, 48

Ostriker J.P., Gnedin O.Y., 1997, ApJ, 487, 667

Secker J, 1992, AJ, 104, 1472

van den Bergh S., 1995, AJ, 110, 1171

Vesperini E., 1994, Ph.D. Thesis, Scuola Normale Superiore, Pisa

Vesperini E., 1997, MNRAS, 287, 915

Vesperini E., Heggie D.C., 1997, MNRAS, 289, 898

Vietri M., Pesce E., 1995, ApJ, 442, 618

Whitmore B.C., Schweizer F., 1995, AJ, 109, 960

Wielen R., 1988, in The Harlow-Shapley Symposium on Globular Cluster Systems in Galaxies, ed. J.E. Grindlay & A.G.D. Philip, IAU Symp. 126 (Dordrecht, Reidel) p.393

Zinn R., 1985, ApJ, 293, 424

 Table 1a

 Effects of evolutionary processes

 on the parameters of the mass function of a globular cluster system

#	process	σ	$< \log M >$
Ι	disruption by evaporation	↓	1
II	disruption by dynamical friction	$\downarrow$	$\downarrow$
III	mass loss of individual surviving clusters	Î	$\downarrow$

A log-normal GCMF with dispersion  $\sigma$  and mean value  $\langle \log M \rangle$  is assumed. The third and the fourth column indicate the effect on  $\sigma$  and  $\langle \log M \rangle$  respectively if the corresponding process indicated in the second column were the only one determining the evolution of the GCMF.

 $\begin{tabular}{ll} \begin{tabular}{ll} Table 1b \\ \end{tabular} Evolution of the parameters of the GCMF \end{tabular} \end{tabular}$ 

$<\log M>_f - <\log M>_i$	$\sigma_f - \sigma_i$	balance of evolutionary effects
< 0 < 0 > 0 > 0	< 0 > 0 < 0 > 0	$ \begin{array}{c} II_M + III_M > I_M; \ I_{\sigma} + II_{\sigma} > III_{\sigma} \\ II_M + III_M > I_M; \ I_{\sigma} + II_{\sigma} < III_{\sigma} \\ II_M + III_M < I_M; \ I_{\sigma} + II_{\sigma} > III_{\sigma} \\ II_M + III_M < I_M; \ I_{\sigma} + II_{\sigma} < III_{\sigma} \end{array} $

I, II, III indicate the effect on the dispersion (subscript  $\sigma$ ) and on the mean value (subscript  $< \log M >$ ) of the GCMF of the three evolutionary processes as indicated in Table 1a

Comparison with observational data						
	Observ.	$\mathrm{Theor}_{no-ds}$	$Theor_{ds}$			
$\langle \log M \rangle$	$5.10\pm0.06$	4.99	5.02			
σ	$0.56\pm0.04$	0.65	0.67			
$\Delta \langle \log M \rangle_{in-out}$	$0.16\pm0.09$	0.07	0.12			
$\Delta \sigma_{in-out}$	$-0.09\pm0.06$	-0.07	-0.06			
$F_D$	$0.038 \pm 0.02$	0.036	0.036			
$F_N$	_	0.54	0.48			
$F_M$	_	0.41	0.38			

 Table 2

 Comparison with observational data

Observational values of  $\langle \log M \rangle$ ,  $\sigma$  are from Gnedin (1997) (assuming  $M/L_V = 2$ ),

 $\Delta \langle \log M \rangle_{in-out}$  and  $\Delta \sigma_{in-out}$  are taken from Ostriker & Gnedin (1997).

The observational value of  $F_D$  is taken from Hut & Djorgovski (1992). Theor<sub>no-ds</sub> indicates the theoretical values estimated without the

Theor<sub>no-ds</sub> indicates the t effects of disk shocking.

Theor $_{ds}$  indicates the theoretical values estimated with the effects of disk shocking.

#### FIGURE CAPTIONS

Figure 1 (a) Dispersion  $\sigma_i$  and mean value of  $\log M$ ,  $\langle \log M \rangle_i$ , of the initial log-normal GCMFs investigated in this paper; (b) final (at t = 15 Gyr) values of  $\sigma$ ,  $\sigma_f$ , and of  $\langle \log M \rangle$ ,  $\langle \log M \rangle_f$ , from the set of initial conditions shown in (a).

Figure 2 Contour plots in the plane  $\sigma_i - \langle \log M \rangle_i$  of  $\langle \log M \rangle_f - \langle \log M \rangle_i$  (a),  $\sigma_f - \sigma_i$  (b),  $\langle \log M \rangle_f$  (c),  $\sigma_f$  (d).

Figure 3 Initial values of  $\sigma_i$  and  $\langle \log M \rangle_i$  for which  $\sigma_f = \sigma_i$  (dashed line) and initial values of  $\sigma_i$  and  $\langle \log M \rangle_i$  for which  $\langle \log M \rangle_f = \langle \log M \rangle_i$  (solid line). These two lines divide the space of initial conditions in four regions, each one characterized by a different evolution of the parameters of the GCMF (see discussion in the text). The point of intersection of the two lines corresponds to an "equilibrium" initial GCMF whose parameters do not evolve even though a significant number of clusters are disrupted in a Hubble time (see text).

Figure 4 Initial (dashed lines) and final (dots and solid lines) GCMF for (a)  $\sigma_i = 0.9$ ,  $\langle \log M \rangle_i = 4.6$ , (b)  $\sigma_i = 0.9$ ,  $\langle \log M \rangle_i = 5.8$ , (c)  $\sigma_i = 0.64$ ,  $\langle \log M \rangle_i = 4.93$ . Dots show the real GCMF obtained at t = 15 Gyr while solid lines show the gaussian distributions with mean value and dipersion estimated from the sample of surviving clusters as discussed in sect.2. Figure 5 Distribution of the initial values of the mass of those clusters which have  $\log M$  at t = 15 Gyr approximately equal to  $\langle \log M \rangle_f$  (in the range  $\langle \log M \rangle_f \pm 0.03$ ). The initial GCMF is a log-normal distribution with  $\sigma = 0.64$  and  $\langle \log M \rangle = 4.93$  (E-GCMF see text).

Figure 6 Difference,  $\Delta \langle \log M \rangle_{in-out}$  between the final value of  $\langle \log M \rangle$  of inner clusters ( $R_g < 8$  Kpc) and that of outer clusters ( $R_g > 8$  Kpc) versus the initial mean value of the GCMF.

Figure 7  $\Delta \langle \log M \rangle_{in-out}$  versus the difference between the final and the initial value of  $\langle \log M \rangle$  for all clusters.

Figure 8  $\Delta \sigma_{in-out}$  versus the initial dispersion of the GCMF  $\sigma_i$ .

Figure 9 Initial (solid line) and final histogram of  $R_g$  for three different initial GCMF:  $\sigma_i = 0.9$ ,  $\langle \log M \rangle_i = 4.6$  (dotted line);  $\sigma_i = 0.7$ ,  $\langle \log M \rangle_i = 5$  (short-dashed line);  $\sigma_i = 0.9$ ,  $\langle \log M \rangle_i = 5.8$  (long-dashed line).

Figure 10 (a)  $\langle \log M \rangle$  at t = 15 Gyr for clusters in five radial bins versus galactocentric distance of the bin for the following initial conditions  $\sigma_i = 0.9$ ,  $\langle \log M \rangle_i = 4.6$  (filled dots);  $\sigma_i = 0.7$ ,  $\langle \log M \rangle_i = 5$  (open circles);  $\sigma_i = 0.9$ ,  $\langle \log M \rangle_i = 5.8$  (triangles). (b)  $\sigma$  at t = 15 Gyr for clusters in five radial bins versus galactocentric distance of the bin. (symbols as in (a)). Figure 11 Same as figure 10 (a) for the initial condition  $\sigma_i = 0.9$ ,  $\langle \log M \rangle_i = 4.6$  but excluding the low-mass tail of the GCMF at t = 15 Gyr. (the values for the entire sample already shown in figure 10 (a) are plotted as filled dots for ease of comparison). Figure 12 Time evolution of  $\langle \log M \rangle$  (a) ,  $\sigma$  (b) and of the ratio of the total number of clusters at time t to the total initial

number of clusters, N(t)/N(0) (c) for initial log-normal GCMF with  $\langle \log M \rangle_i = 4.5$  and  $\sigma_i = 1$  (circles) and with  $\langle \log M \rangle_i = 6$  and  $\sigma_i = 1$  (triangles).

Figure 13 Trajectories in the plane  $\sigma$ - $\langle \log M \rangle$  (see sect.3.4 for a detailed comment on the figure)

Figure 14 Contour plot in the plane  $\sigma_i - \langle \log M \rangle_i$  of the ratio,  $F_N$ , of the total number of clusters surviving after 15 Gyr to the total initial number of clusters (a), and of the ratio,  $F_M$ , of the total mass of all surviving clusters after 15 Gyr to the total initial mass of all clusters (b).

Figure 15 Contour plot in the plane  $\sigma_i - \langle \log M \rangle_i$  of the current value of cluster disruption rate (see text for definition).

Figure 16 Contour plot of the core radius,  $R_c$ , of the spatial distribution (at t = 15 Gyr) of clusters in the Galaxy in the plane  $\sigma_i - \langle \log M \rangle_i$ .

Figure 17 Final values of  $\langle \log M \rangle$  (a),  $\sigma$  (b),  $F_N$  (c),  $F_D$  (d) from the simulations without the effects of disk shocking versus those obtained taking into account disk shocking.

Figure 18 Initial and final GCMF for a simulation starting with a power-law GCMF with  $\alpha = 2$  and  $M_{low} = 10^4 M_{\odot}$ . Dots show the real GCMF obtained at t = 15 Gyr while solid line shows the gaussian distribution with mean value and dipersion estimated from the sample of surviving clusters as discussed in sect.2. Dashed line shows the initial GCMF.

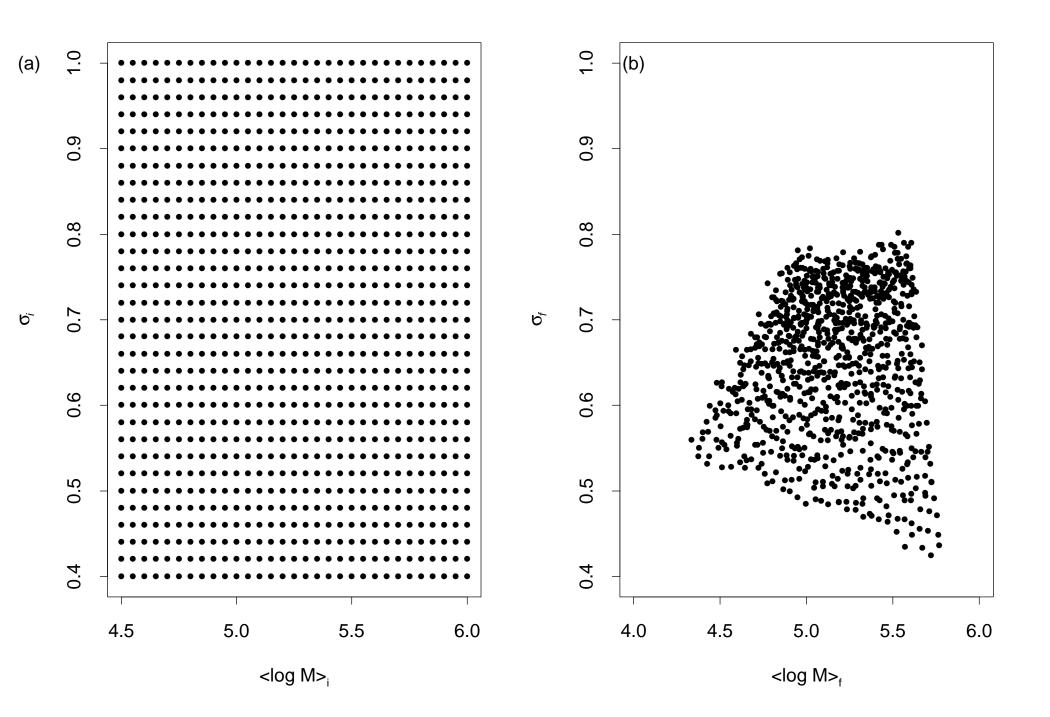
Figure 19 Final values of  $(\log M)$  (a) and  $\sigma$  (b) versus the low-mass cutoff in the initial GCMF for systems with a power-law initial GCMF,  $f(M) \propto M^{-\alpha}$ .  $\alpha = 2$  (filled dots),  $\alpha = 1.7$  (triangles ),  $\alpha = 1.5$  (crosses).

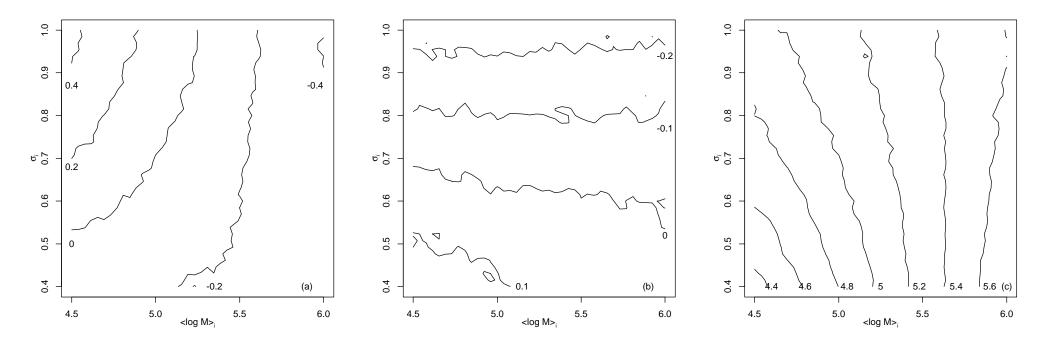
Figure 20 Histogram of the ratio of the final to initial mass for clusters surviving after one Hubble time in a system with an initial log-normal GCMF with ( $\langle \log M \rangle_i = 5.0, \sigma_i = 0.7$ ). (N(15) is the total number of clusters survived at t = 15 Gyr)

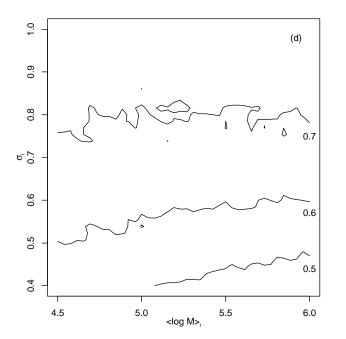
Figure 21 (a) Histogram of  $\log[t_d(t_H)/t_H]$  (where  $t_d(t_H)$  is the disruption timescale of a cluster at  $t_H = 10$  Gyr) for the sample of clusters surviving at  $t = t_H$  from an initial population with a log-normal GCMF (with  $\sigma_i = 0.7$  and  $\langle \log M \rangle_i = 5.0$ ). The dashed line is the fit to the histogram assuming the initial distribution of  $t_d$  to be a power-law while the solid line is the resulting distribution at  $t = t_H$  adopting the real initial distribution of  $t_d$  (see panel (b)) which is a log-normal distribution. (b) Histogram of the initial values of  $\log t_d$  for the system of clusters with an initial log-normal GCMF (with  $\sigma_i = 0.7$  and  $\langle \log M \rangle_i = 5.0$ ). The solid line shows the best fit log-normal distribution ( $\sigma = 0.67$ ,  $\langle \log[t_d(0)/t_H] \rangle = 0.15$ ).

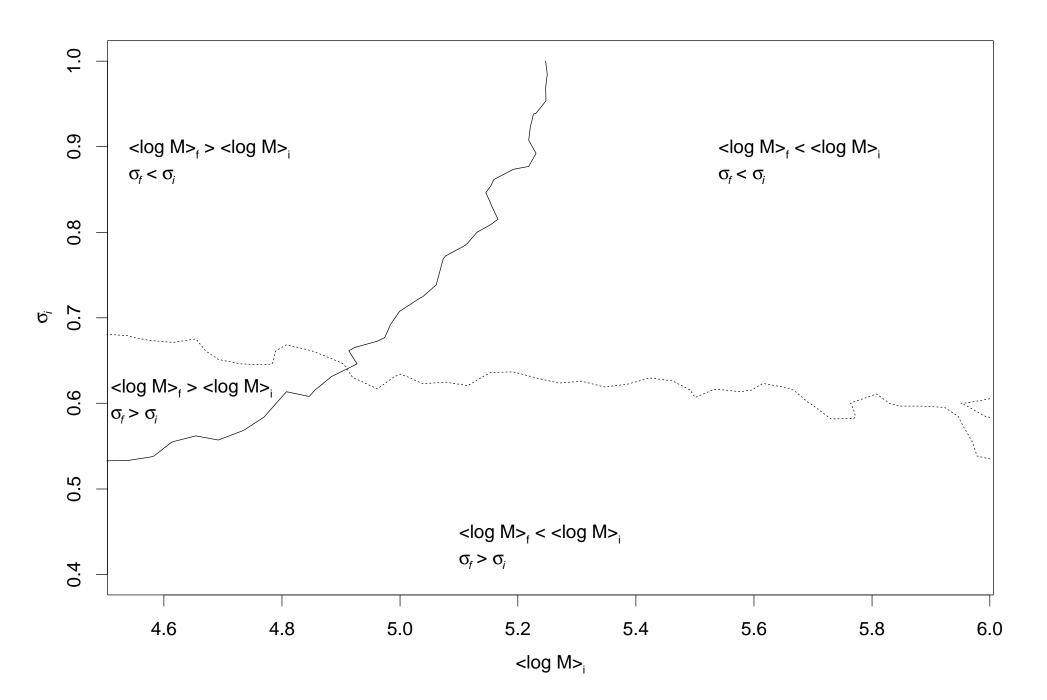
Figure 22 Initial (t = 0) and final (at t = 10 Gyr) distribution of  $\log t_d/t_H$  for three different systems: short dashed lines show the initial (upper curve) and final (lower curve) distributions for a system with an initial log-normal distribution of  $t_d$  with  $(\sigma = 1.0, \langle \log[t_d(0)/t_H] \rangle = -0.7)$ ; solid lines (initial distribution is the upper curve and final distribution is the lower curve) correspond to a system with an initial log-normal distribution of  $t_d$  with ( $\sigma = 0.67, \langle \log[t_d(0)/t_H] \rangle = 0.15$ ); long dashed lines (initial distribution is the upper curve and final distribution is the lower curve) correspond to a system with an initial

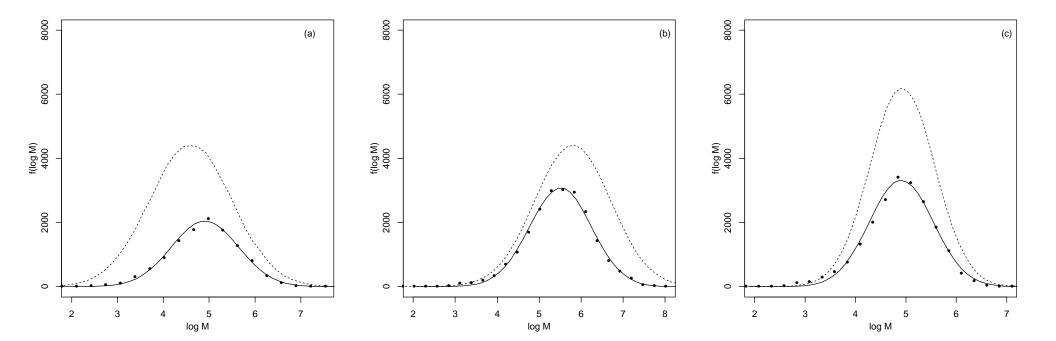
power-law distribution of  $t_d$ ,  $f_i \sim t_d^{-q}$ , with q = 1.6. The normalizations of the initial distributions have been chosen so to have the same total number of surviving clusters in the final samples at  $t = t_H$ .

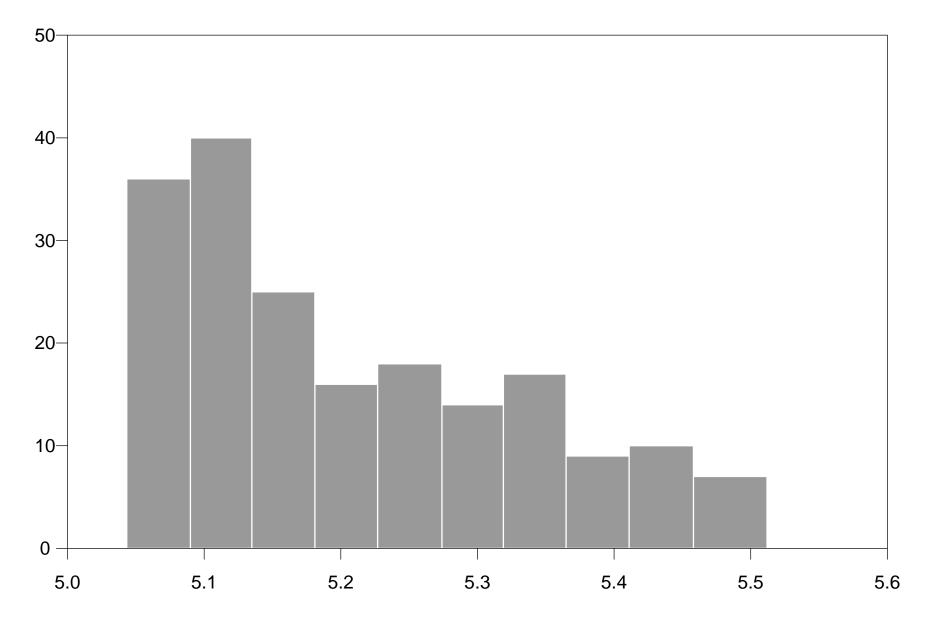




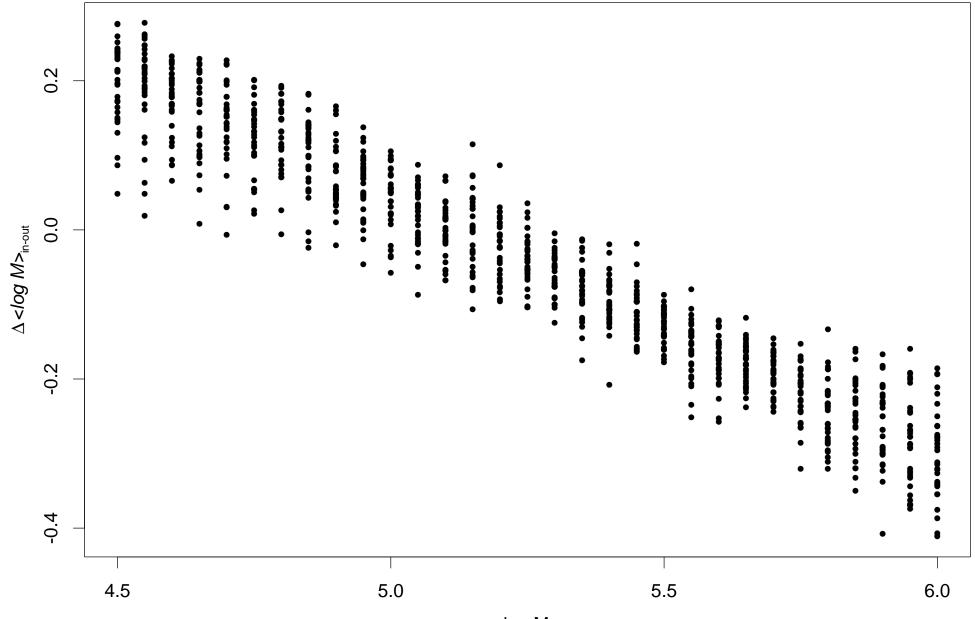




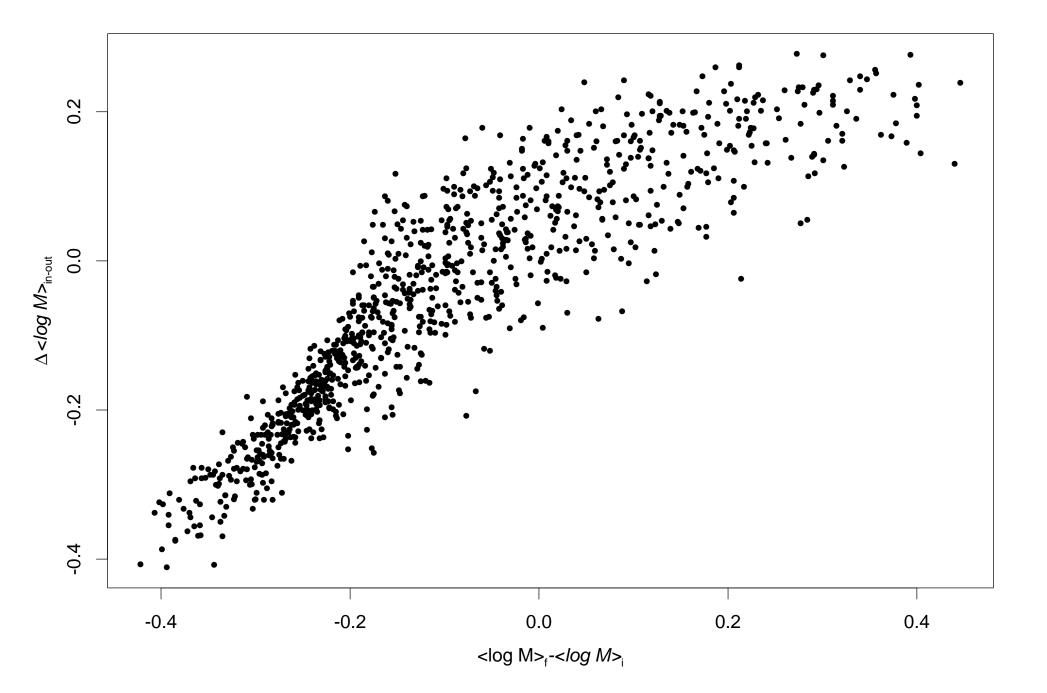


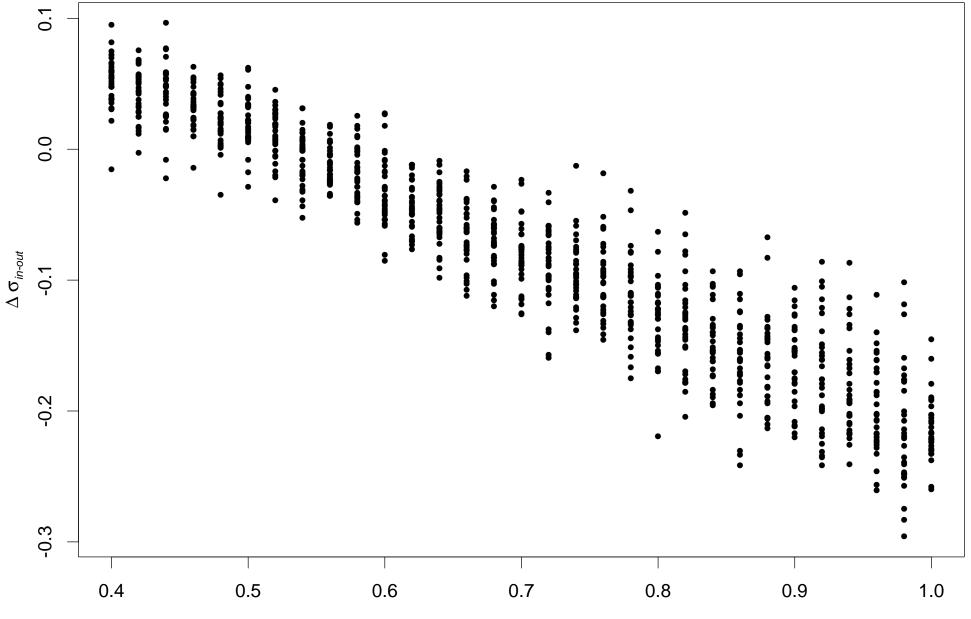


 $\log M_{\rm i}$ 

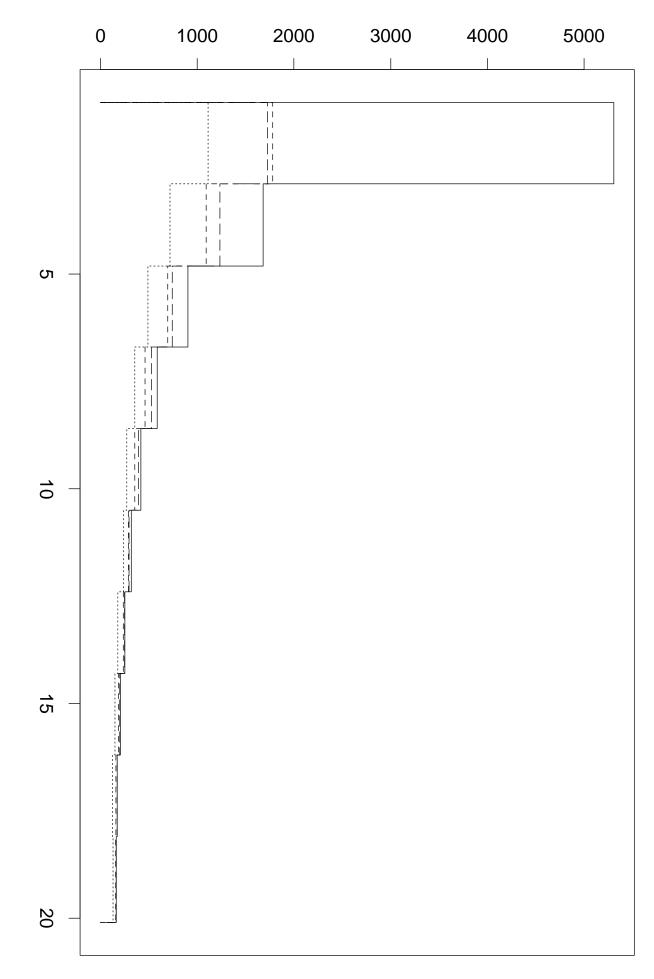


<log M><sub>i</sub>



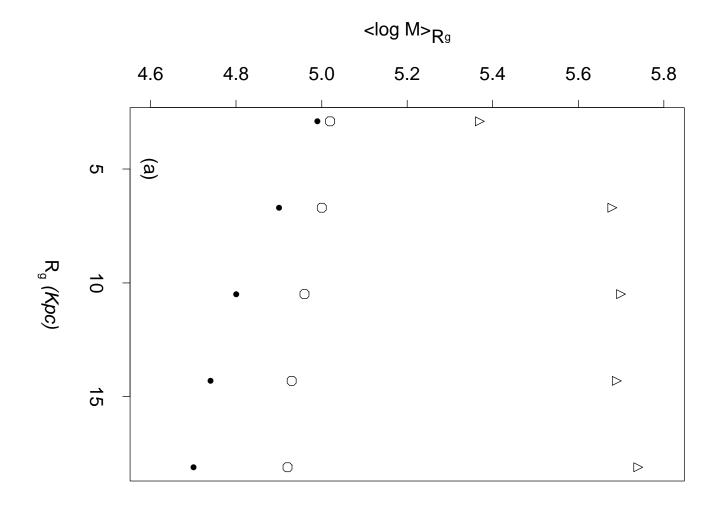




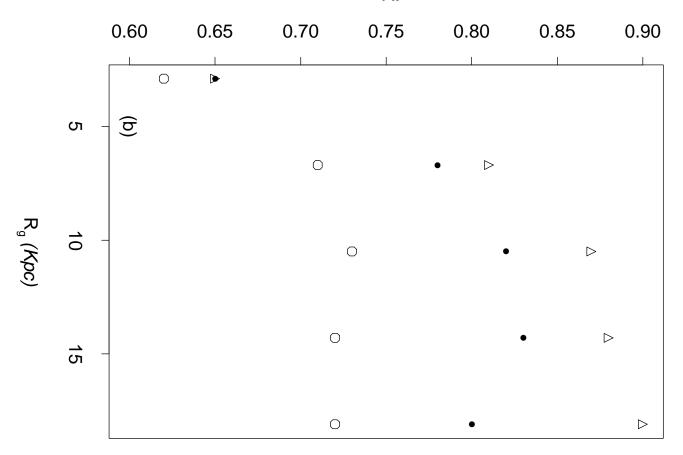


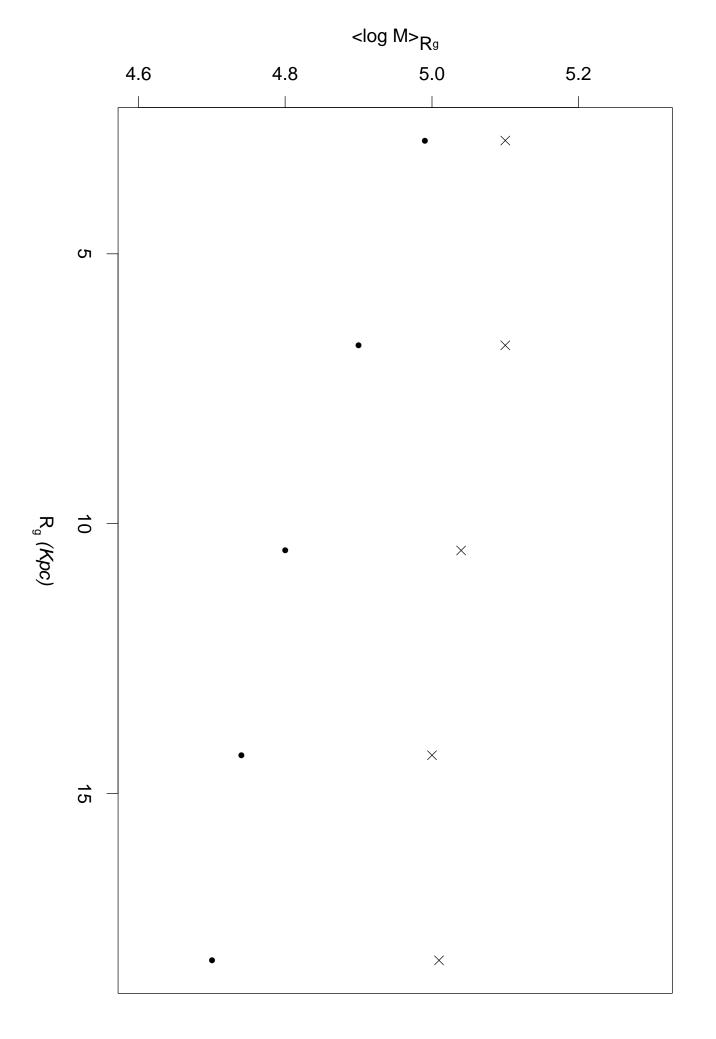
R<sub>g</sub> (Kpc)

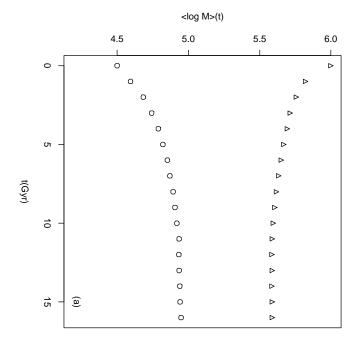
Ν

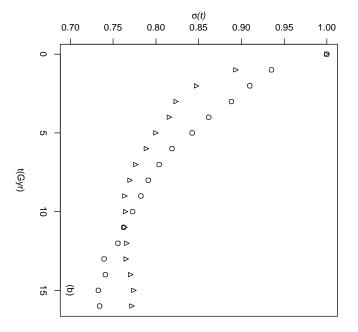






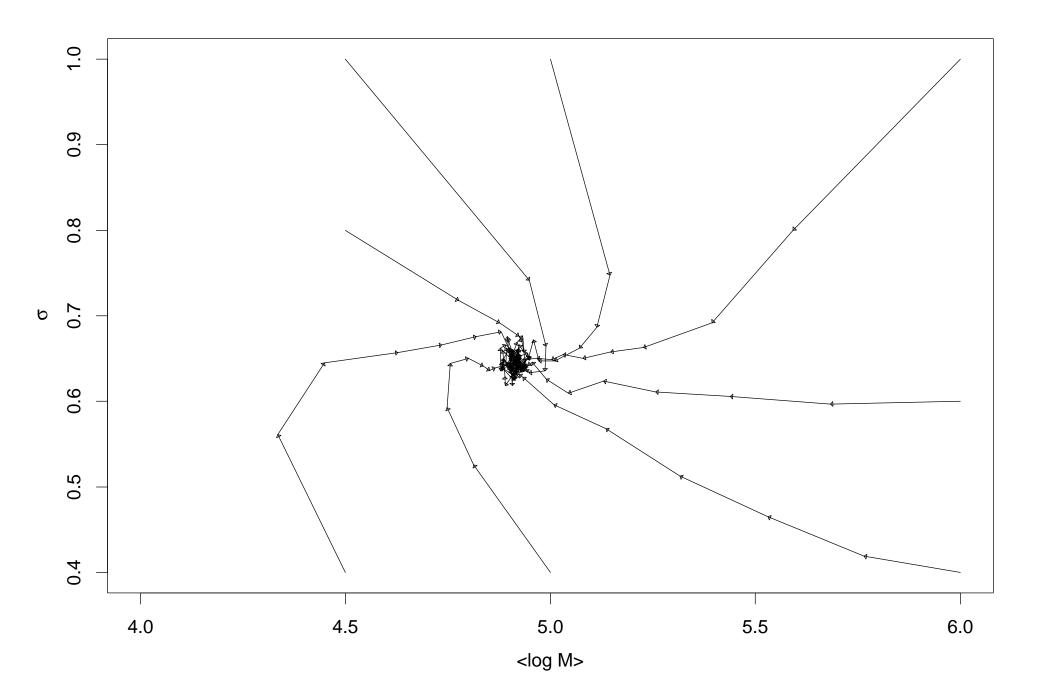


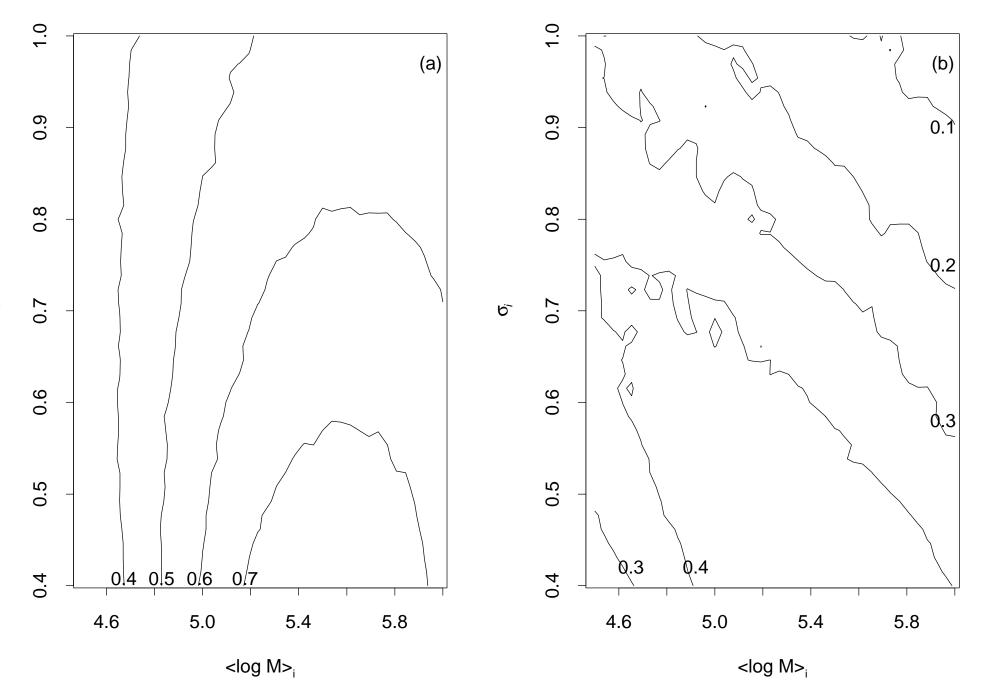


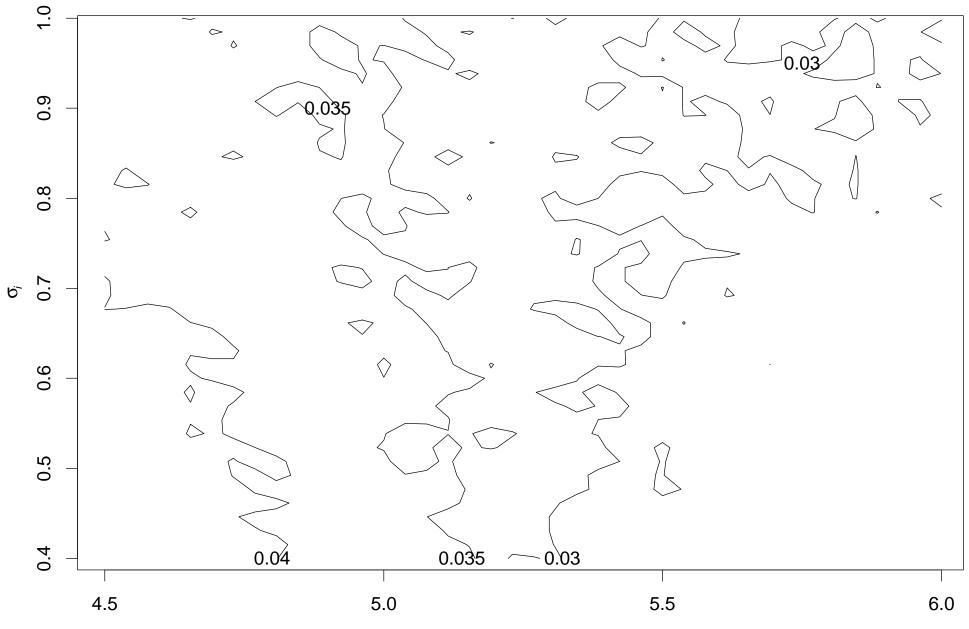


N(t)/N(0) 0.2 0.4 0.6 0.8 1.0 1 0 Ø 0 ⊳ Þ 0 Ο СЛ ο О ⊳ 0 ⊳ о ⊳ 0 ⊳ 10 0 ⊳ 0 ⊳ 0 ⊳ 0 ⊳ 0 ⊳ 15 (c) 0 ⊳ о ⊳

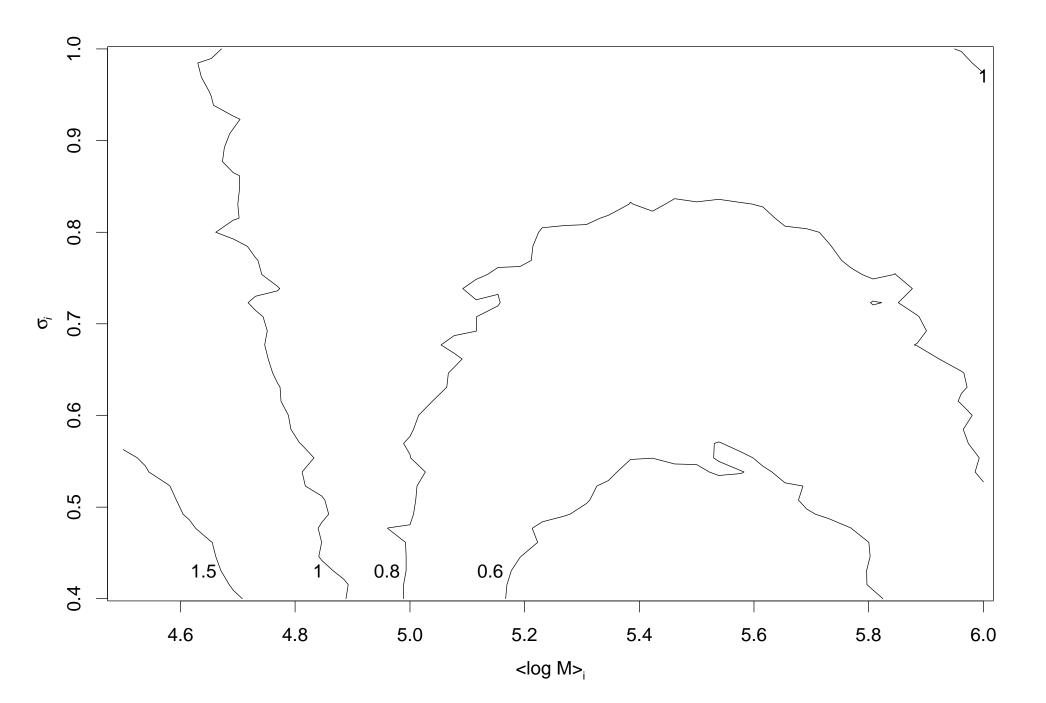
t(Gyr)

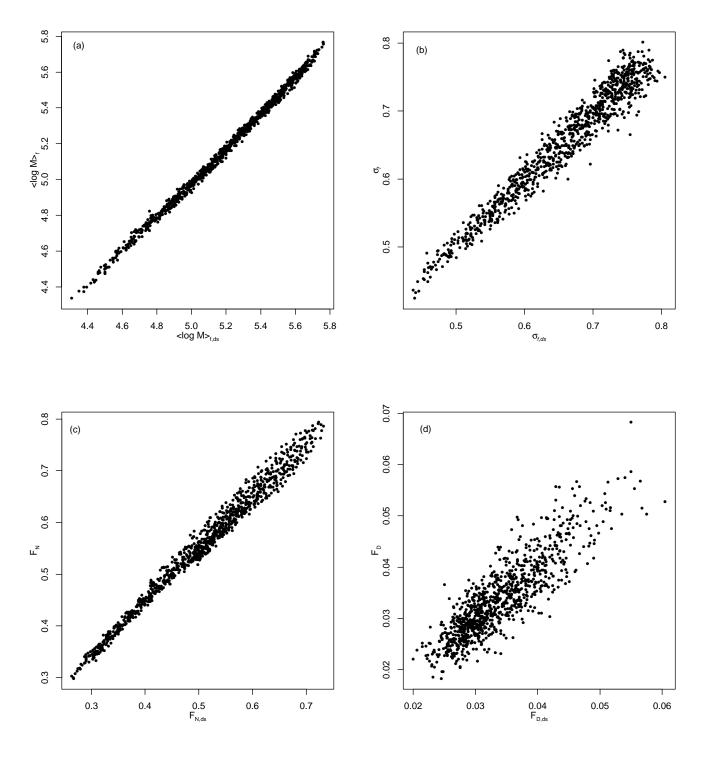


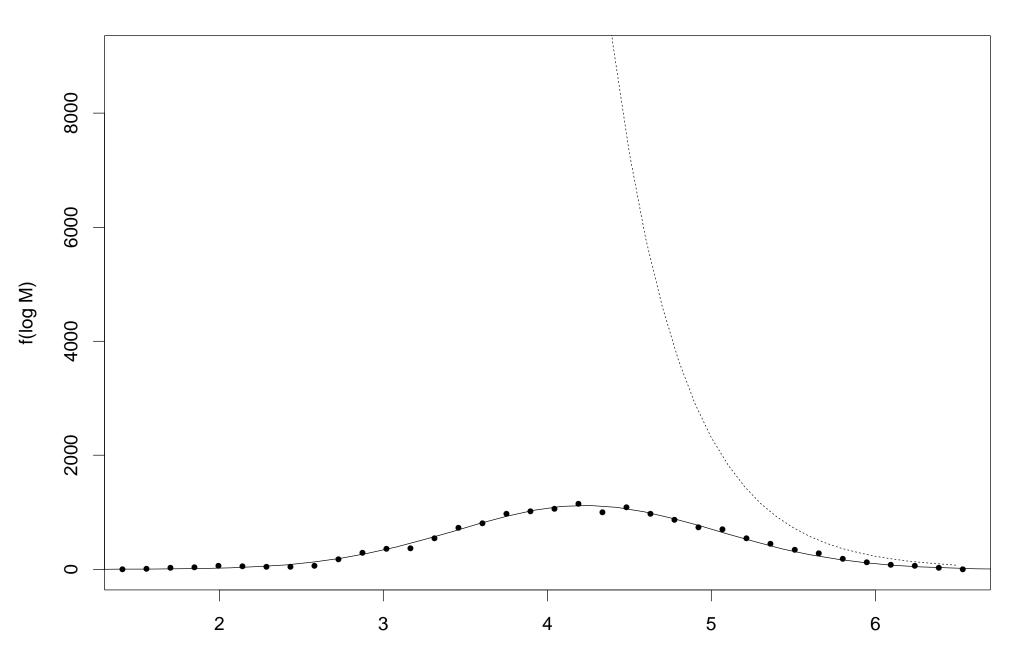




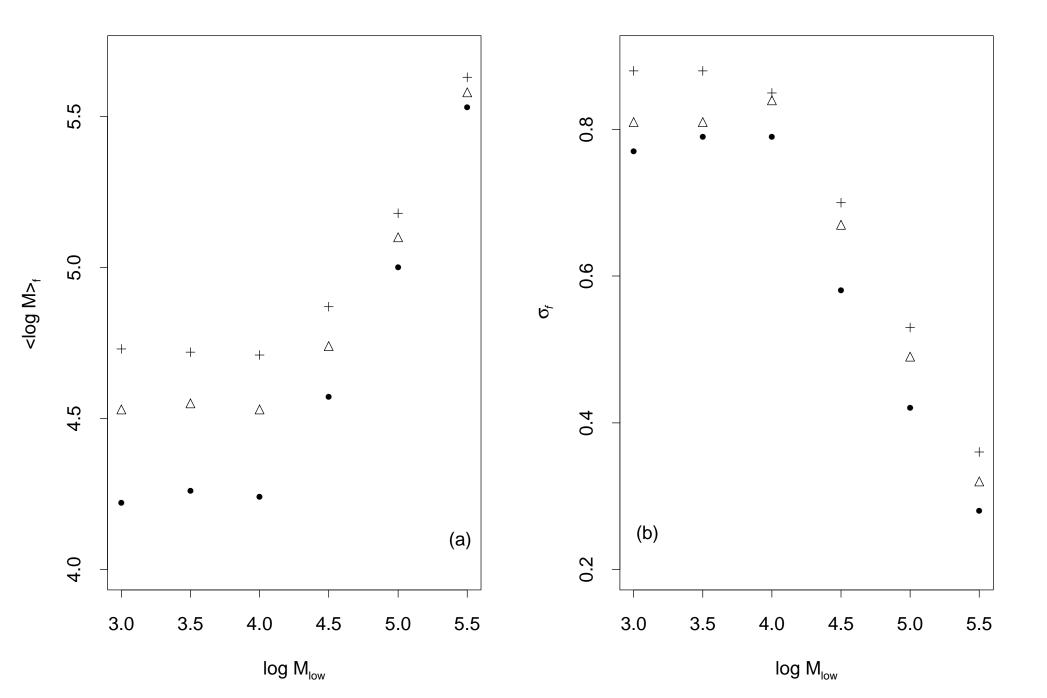
<log M><sub>i</sub>

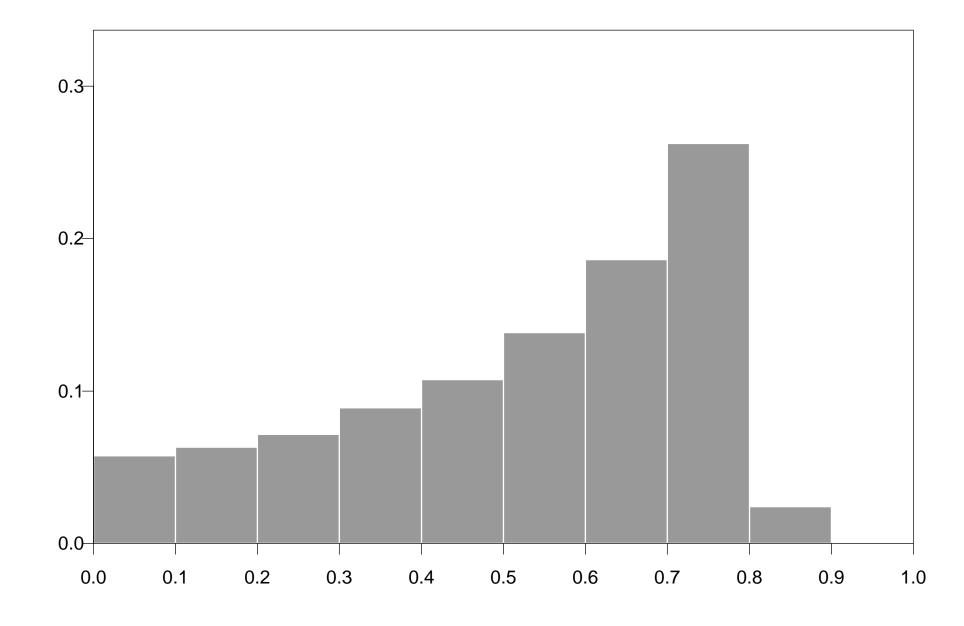




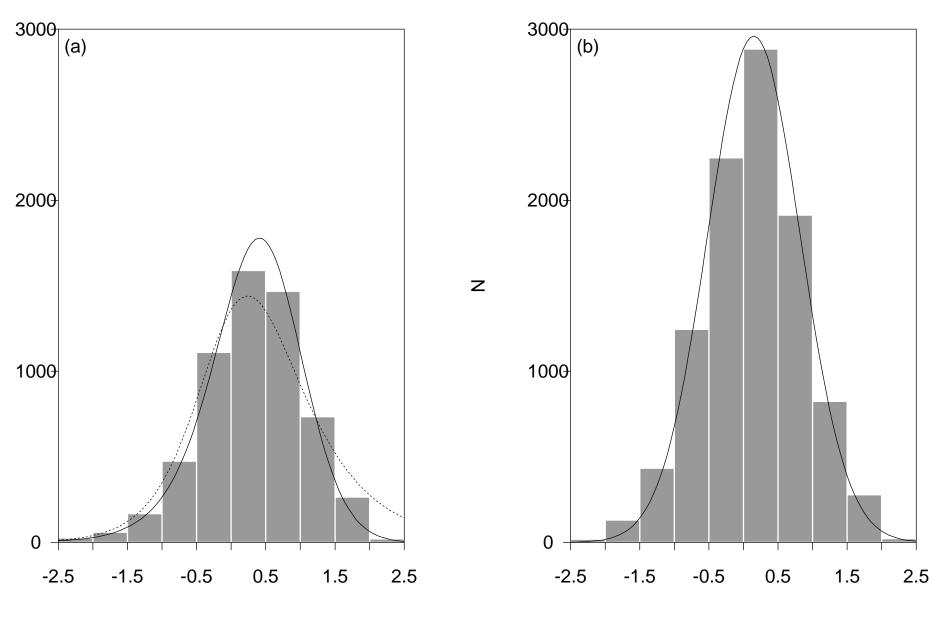


log M





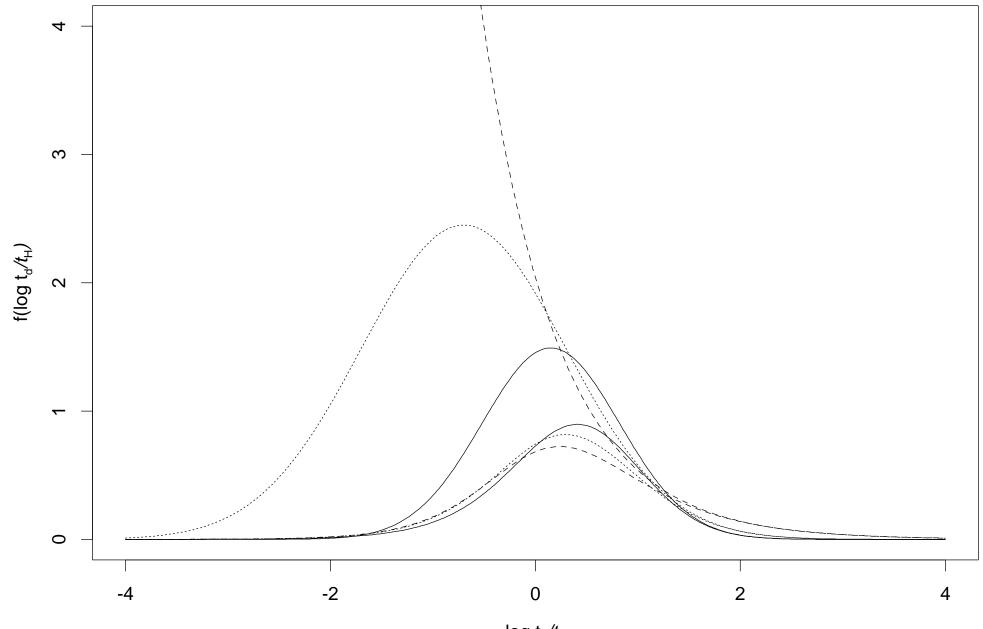
N/N(15)



 $\log t_d / t_H$ 

Ζ

 $\log t_d/t_H$ 



 $\log t_d / t_H$